



# Tectonic events reflected by palaeocurrents, zircon geochronology, and palaeobotany in the Sierra Baguales of Chilean Patagonia



Nestor M. Gutiérrez<sup>a</sup>, Jacobus P. Le Roux<sup>a,b,\*</sup>, Ana Vásquez<sup>a,c</sup>, Catalina Carreño<sup>a,d</sup>, Viviana Pedroza<sup>a</sup>, José Araos<sup>a,e</sup>, José Luis Oyarzún<sup>f</sup>, J. Pablo Pino<sup>g</sup>, Huber A. Rivera<sup>a,b</sup>, L.F. Hinojosa<sup>g,h</sup>

<sup>a</sup> Departamento de Geología, FCFM, Universidad de Chile, Plaza Ercilla 803, Santiago, Chile

<sup>b</sup> Centro de Excelencia en Geotermia de los Andes, Plaza Ercilla 803, Santiago, Chile

<sup>c</sup> FCC Servicios Ciudadanos, Av. Vitacura 2771, Of. 403, Santiago, Chile

<sup>d</sup> Codelco, Calama, Chile

<sup>e</sup> Departamento de Geografía, Facultad de Cs. Sociales, Universidad Alberto Hurtado, Cienfuegos 41, Santiago, Chile

<sup>f</sup> Miraflores 863, Puerto Natales, Chile

<sup>g</sup> Instituto de Ecología y Biodiversidad (IEB), Santiago, Chile

<sup>h</sup> Departamento de Ciencias Ecológicas, Universidad de Chile, Ñuñoa, Santiago, Chile

## ARTICLE INFO

### Article history:

Received 23 August 2016

Received in revised form 6 December 2016

Accepted 9 December 2016

Available online 13 December 2016

### Keywords:

Andean tectonics

Patagonian Transgression

Zircon provenance

Gondwana reconstruction

Antarctic Peninsula

## ABSTRACT

The Sierra Baguales, situated north of the Torres Del Paine National Park in the Magallanes region of southern Chile, shows a well-exposed stratigraphic sequence ranging from the Late Cretaceous to late Pliocene, which presents a unique opportunity to study the evolution of sedimentological styles and trends, palaeoclimate changes, and tectonic events during this period. The depositional environment changed from a continental slope and shelf during the Cenomanian-Campanian (Tres Pasos Formation) to deltaic between the Campanian-Maastrichtian (Dorotea Formation) and estuarine in the Lutetian-Bartonian (Man Aike Formation). During the Rupelian, a continental environment with meandering rivers and overbank marshes was established (Río Leona Formation). This area was flooded in the early Burdigalian (Estancia 25 de Mayo Formation) during the Patagonian Transgression, but emerged again during the late Burdigalian (Santa Cruz Formation). Measured palaeocurrent directions in this Mesozoic-Cenozoic succession indicate source areas situated between the northeast and east-southeast during the Late Cretaceous, east-southeast during the middle Eocene, and southwest during the early Oligocene to early Miocene. This is confirmed by detrital zircon age populations in the different units, which can be linked to probable sources of similar ages in these areas. The east-southeastern provenance is here identified as the Antarctic Peninsula or its northeastern extension, which is postulated to have been attached to Fuegian Patagonia during the Eocene. The southwestern and western sources were exhumed during gradual uplift of the Southern Patagonian Andes, coinciding with a change from marine to continental conditions in the Magallanes-Austral Basin, as well as a decrease in mean annual temperature and precipitation indicated by fossil leaves in the Río Leona Formation. The rain shadow to the east of the Andes thus started to develop here during the late Eocene-early Oligocene (~34 Ma), long before the "Quechua Phase" of Andean tectonics (19–18 Ma) that is generally invoked for its evolution at lower latitudes.

© 2016 Elsevier B.V. All rights reserved.

## 1. Introduction

The Southern Patagonian Andes resulted from collision of the Nazca Plate with southernmost South America, which was manifested in various pulses of uplift during the Late Cretaceous, Eocene and late Miocene (Ramos and Kay, 1992; Ramos, 2005). Such changes in the source topography can have important effects on hydrodynamic conditions and sedimentation styles within the adjoining depocenters (Ruddiman

et al., 1997; Bossi et al., 2000), which in this case are represented by the Magallanes-Austral Basin (Fig. 1A).

The link between Andean tectonics and the sedimentology of Cenozoic successions in the Magallanes-Austral Basin has only been partially investigated to date. Palaeocurrent measurements in the Última Esperanza Province of Patagonia have been restricted mostly to the Upper Cretaceous Cerro Toro and Dorotea Formations (Scott, 1966; Fildani and Hessler, 2005; Crane and Lowe, 2008; Romans et al., 2010; Schwartz and Graham, 2015), the middle – upper Eocene Man Aike Formation (Le Roux et al., 2010), and the lower Miocene Santa Cruz Formation (Bostelmann et al., 2013). Similarly, relatively few zircon ages have been published (Bernhardt, 2011; Fosdick et al., 2011, 2015a, 2015b;

\* Corresponding author at: Departamento de Geología, FCFM, Universidad de Chile, Plaza Ercilla 803, Santiago, Chile.

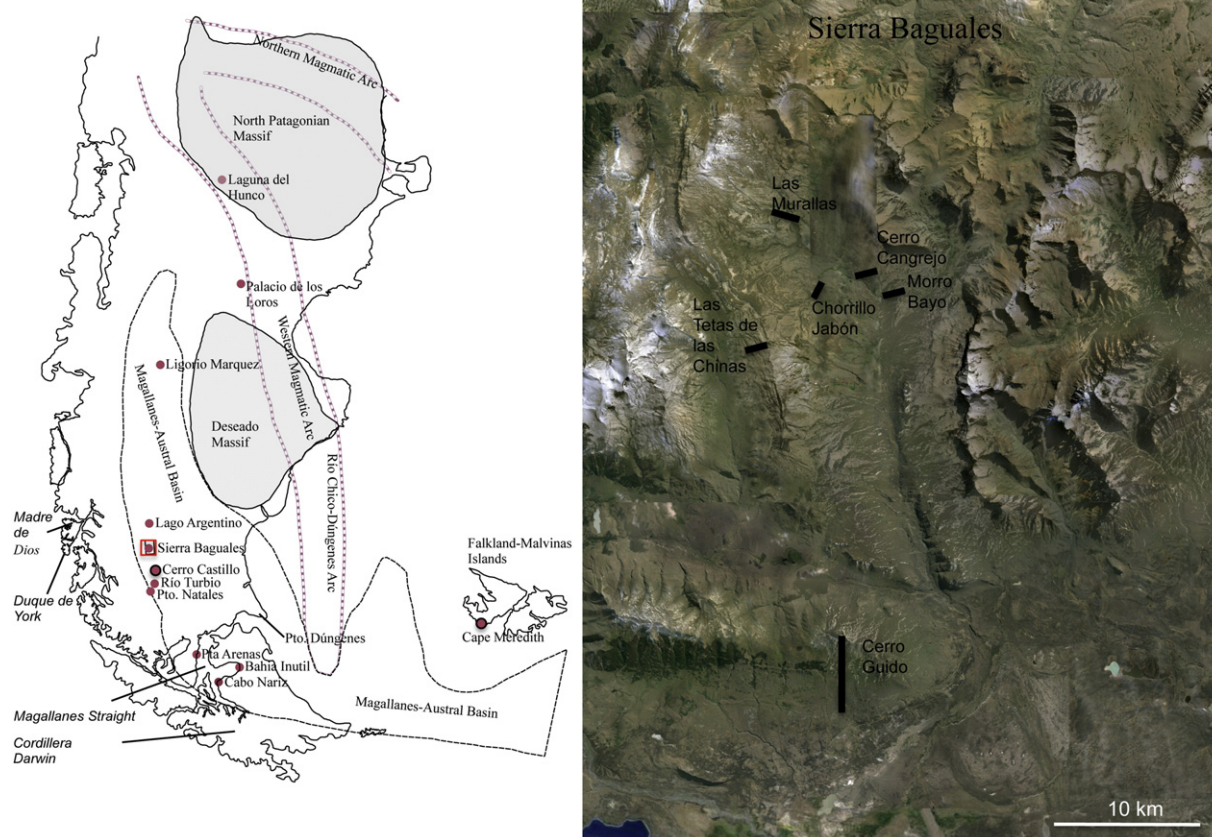


Fig. 1. Locality map of South America and the Sierra Baguales showing tectonic elements and Tertiary fossil leaf localities.

Bostelmann et al., 2013; Schwartz et al., 2016, and references therein), and only one provenance study based on zircon populations was carried out for the post-Cretaceous formations in the southernmost part of the basin (Barbeau et al., 2009). A comprehensive provenance study based on zircon populations has therefore been lacking for the post-Cretaceous formations. As a result, most previous authors (e.g., Bernhardt et al., 2008; Hubbard et al., 2010; Cuitiño, 2011; Schwartz and Graham, 2015) considered the provenance areas of the Magallanes-Austral Basin to have been located to the north, west, and southwest (Barbeau et al., 2009; Zahid and Barbeau, 2010) thus ignoring the existence of possible sources to the east.

In the Sierra Baguales, located about 100 km north of Puerto Natales (Fig. 1A), the stratigraphic succession includes all the formations mentioned above as well as the Rupelian Estancia 25 de Mayo Formation, but with the exception of the Cerro Toro Formation. In spite of previous studies in this and surrounding areas (Feruglio, 1938; Piatnitzky, 1938; Cecioni, 1957; Hoffstetter et al., 1957; Furque, 1973; Malumián, 1990; Marensi et al., 2000, 2002, 2005; Le Roux et al., 2010; Malumián and Nañez, 2011; Cuitiño et al., 2012; Bostelmann et al., 2013), there has been no consensus about the geographic distribution of the different stratigraphic units and their contact relationships. For the Sierra Baguales, in fact, the most detailed geological map presently existing is at a scale of 1:100,000, showing obsolete nomenclature such as the “Río Bandurrias”, “Calafate” and “Las Flores” Formations (Muñoz, 1981). Here we present a new geological map at a scale of 1:10,000 (Fig. 2), updating the nomenclature according to international stratigraphic principles and correcting the spatial distribution of the different stratigraphic units. However, our main objective has been to determine the link between sedimentation in the Magallanes-Austral Basin and its tectonic context. With this in mind, we investigated the depositional environments of the different units and their palaeocurrent patterns, backed up by a study of zircon age populations. Six new detrital zircon

U-Pb ages are presented, of which three are from the Dorotea Formation, one from the Man Aike Formation, and two from the Río Leona Formation. Bearing in mind the well-established relationship between tectonics and local climate, we also carried out a palaeobotanical analysis based on fossils leaves from the Río Leona Formation, comparing these results with those of similar studies on older successions in Patagonia.

## 2. Methodology

Field work in the Sierra Baguales consisted of geological mapping, the measurement of stratigraphic columns and palaeocurrent directions, sampling for petrographic work and detrital zircon dating, and the collection of fossil leaves for palaeobotanical and palaeoclimatic studies.

Geological mapping of the Sierra Baguales was carried out on a scale of 1:10,000 between Cerro Cono in the north, Cerro Ciudadela and the Chilean-Argentinean border in the east, Cerro Guido in the south, and the Río Las Chinas in the west (Fig. 2).

Seven stratigraphic columns (some composite) were measured at 10 different localities (Fig. 1B). In the Tres Pasos Formation, a 380 m thick composite section was surveyed at Cerro Guido and Estancia Las Chinas. Towards the west, at Las Tetas de las Chinas, a 200 m thick profile was surveyed in the Dorotea Formation. The stratigraphy of the Man Aike Formation was described in 3 different sections comprising its basal, middle and upper parts, respectively. The basal section, measured in the vicinity of Las Tetas de las Chinas, has a thickness of 40 m, while the middle section comprised 240 m measured by Le Roux et al. (2010) on Estancia 3R, which was correlated with the section described by Ugalde (2014) and Cecioni (1957) in the sector Las Flores. The upper part has a thickness of 50 m measured at Chorrillo Jabón. In the Río Leona Formation, two 115 m thick profiles were surveyed. The basal

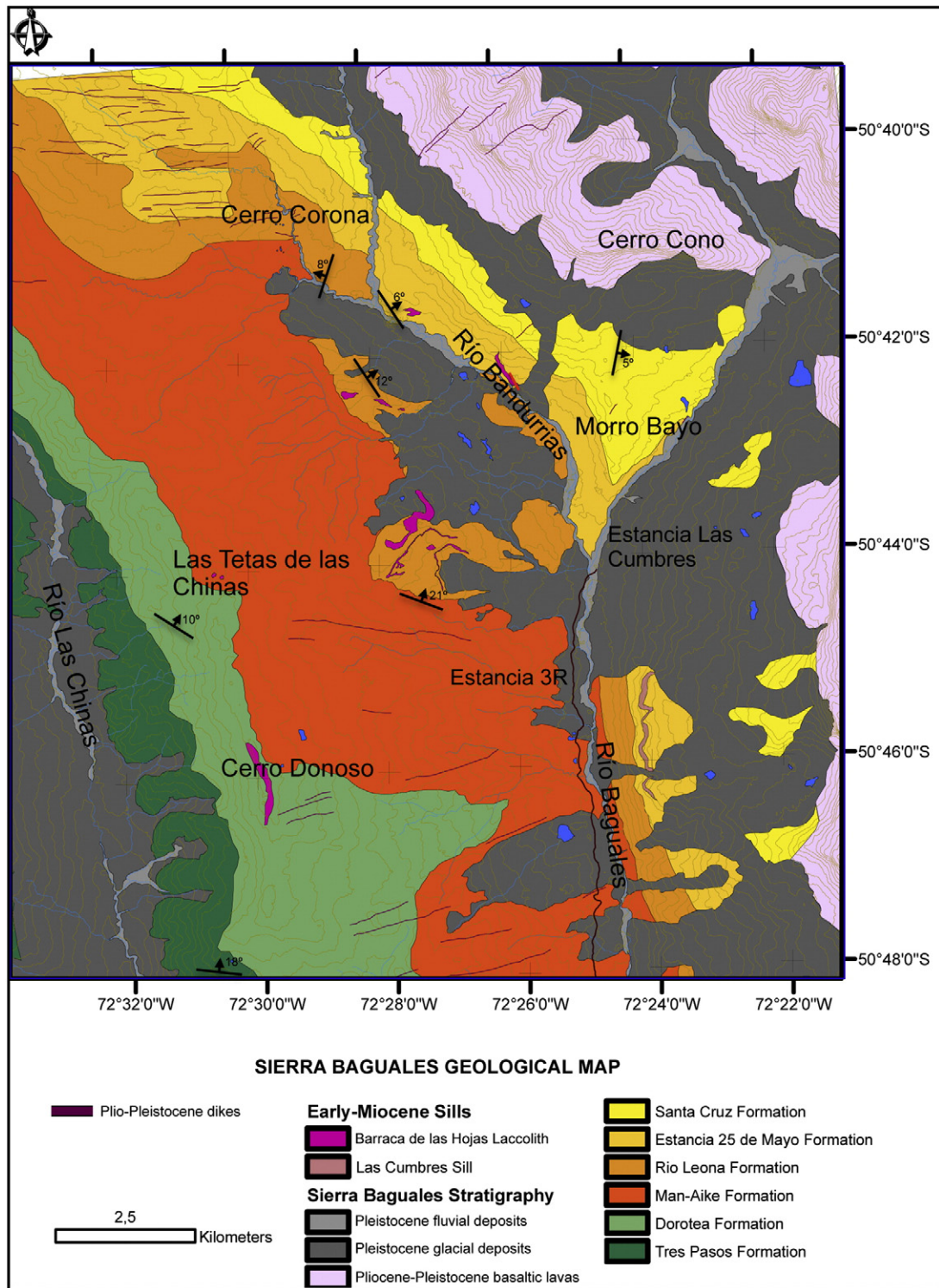


Fig. 2. Geological map of the Sierra Baguales.

part of this formation, which conformably overlies the Man Aike Formation in this area, was measured in the sectors Barranca de las Hojas and Chorrillo Jabón, whereas the upper part was measured at Las Murallas west of the Bandurrias River (Fig. 2). Two stratigraphic columns were also measured in the Estancia 25 de Mayo Formation, the first at the locality of Las Murallas and the second at Cerro Cangrejo. The profile of the Santa Cruz Formation at Cerro Cono, measured by the first four authors of this paper and published in Bostelmann et al. (2013), was included as part of the data base.

A total of 192 palaeocurrent directions were measured, including planar and trough cross-lamination, streaming and parting lineation, rib-and-furrow structures, ripple marks, and the elongation of nodules and concretions where such structures showed a preferred orientation at any particular locality. The growth of concretions is controlled by the grain orientation of their host beds and like streaming and parting lineation do not yield vectors, but can be used in conjunction with other associated structures such as cross-bedding to find the palaeocurrent trends. The recorded directions were distributed as

follows: 55 in the Dorotea Formation, 9 in the Man Aike Formation, 18 in the Río Leona Formation, 37 in the Estancia 25 de Mayo Formation, and 73 in the Santa Cruz Formation. Although the beds in this particular area are generally sub-horizontal, tilt corrections were carried out to obtain the original palaeocurrent directions using the methodology of Le Roux (1991). These were further analyzed by directional statistics (Le Roux, 1992, 1994), to obtain the vector mean azimuth, magnitude, and channel sinuosity of each data set. In the Tres Pasos and Estancia 25 de Mayo Formations no measurable directions were encountered. However, published palaeocurrent data from the Estancia 25 de Mayo Formation at Lago Argentino (Cuitiño, 2011) were also incorporated into this data set.

Eight samples from the Sierra Baguales succession were selected for detrital zircon dating. The first of these was taken from the Dorotea Formation close to its basal contact with the Tres Pasos Formation near Cerro Guido (Fig. 1B), whereas the second and third are from the upper part of the Dorotea Formation at Las Tetes de las Chinas. One sample was dated from near the top of the overlying Man Aike Formation at Chorrillo Jabón (Fig. 1B). For the Río Leona Formation, two samples were dated, one from Chorrillo Jabón close to its basal contact with the Man Aike Formation, and the other from Cerro Ciudadela, where it was previously attributed to the “Las Flores Formation” and correlated with the Man Aike Formation (Ugalde, 2014). These 6 samples were analyzed in the Mass Spectrometry Laboratory of the Andean Geothermal Centre of Excellence (CEGA) at the University of Chile. Two other samples, previously dated at the Australian National University in Canberra (Bostelmann et al., 2012) were collected from near the base and top of the Santa Cruz Formation, respectively.

More than 3700 fossil leaves recovered from the Río Leona Formation were identified, classified, and subjected to multi- and univariate analysis to determine temperature and precipitation conditions as well as their morphospecies diversity. Palaeoclimatic analysis was performed using the models and datasets of Hinojosa and collaborators (Hinojosa, 2005; Hinojosa et al., 2006, 2011).

### 3. Geological setting

The Rocas Verdes Basin, a predecessor of the Magallanes-Austral Basin, developed as a backarc or marginal basin during a Middle to Late Jurassic extensional episode associated with the initial breakup of Gondwanaland (Dalziel et al., 1974; Gust et al., 1985; Biddle et al., 1986; Pankhurst et al., 2000; Calderón et al., 2007). Inversion converted its eastern part into a foreland basin and caused flexural loading, thus creating the north-south orientated Magallanes-Austral Basin (Natland et al., 1974; Dalziel, 1986).

The Sierra Baguales represents the region in the Magallanes-Austral Basin with the most complete, uninterrupted Mesozoic–Cenozoic stratigraphic succession, reaching a total approximate thickness of 1300 m. It includes the Tres Pasos and Dorotea Formations, both of Late Cretaceous age, as well as the Man Aike Formation (middle to late Eocene), Río Leona Formation (early Oligocene), Estancia 25 de Mayo Formation (early Miocene), and the Santa Cruz Formation (middle Miocene).

The basal part of the Tres Pasos Formation is partly contemporaneous with the underlying Cerro Toro Formation, which represents large, conglomerate-filled submarine channels prograding towards the south along the Magallanes-Austral axis (Katz, 1963; Natland et al., 1974; Hubbard et al., 2008). The Tres Pasos Formation is of late Campanian age in its uppermost part, as indicated by the ammonites *Hoplitoplacenticeras plasticus* and *H. semicostatus* at Cerro Cazador (Paulcke, 1907). Its contact with the overlying Dorotea Formation is concordant, as revealed in the upper part of Cerro Guido (Fig. 1B). The latter formation reaches a thickness of about 200 m in the study area, consisting mainly of medium to coarse sandstones. The Man Aike Formation, previously referred to as the Río Baguales or Las Flores Formation in different parts of the study area (Le Roux et al., 2010; Ugalde, 2014), overlies the Dorotea Formation paraconformably to

unconformably, consisting of about 300 m of medium- to coarse-grained sandstones and conglomerates. Apart from fossils clearly reworked from the underlying Dorotea Formation, late Eocene shark teeth, fish fossils and invertebrates are present (Otero et al., 2013). The Río Leona Formation overlies the Man Aike Formation concordantly at Chorrillo Jabón, where it reaches an approximate thickness of 200 m. It is here composed mainly of mudstones and medium-grained sandstones with intraformational conglomerate lenses. Thin lignite beds, as well as fossil wood and leaves are common (Barreda et al., 2009; Torres et al., 2009). The Estancia 25 de Mayo Formation concordantly overlies the Río Leona Formation and represents the Patagonian or “Superpatagonian” Transgression (Feruglio, 1949; Malumián, 1999), which took place during the early Miocene between 20 and 18 Ma (Parras et al., 2012; Bostelmann et al., 2013; Cuitiño et al., 2013). Its fossil assemblage includes oyster banks (*Ostrea hatcheri*), bivalves, typical Leonenses gastropods such as *Perissodonta ameghinoi*, and crabs (*Chaceon peruvianum*) (Gutiérrez et al., 2013). A prominent, 2 m thick pyroclastic horizon of rhyodacitic composition is present in the middle of this unit at Cerro Corona (Figs. 2, 3). It was also reported in the Lago Argentino succession, where it was identified as “LPL” and dated by U–Pb at  $19.14 \pm 0.5$  Ma (Cuitiño et al., 2013). The Santa Cruz Formation lies conformably upon the Estancia 25 de Mayo Formation (Bostelmann et al., 2013) at Cerro Cono (Fig. 2), where it reaches a thickness of about 100 m. It consists of multi-coloured mudstones with medium to coarse sandstones and conglomerates. Terrestrial vertebrate fossils indicate a post-Colhuehuapense to pre-Santacrucian age, which is supported by a population of detrital zircons with a mean age of  $18.23 \pm 0.26$  Ma (Bostelmann et al., 2013). However, the dated sample also contained several zircons with ages of about 16 Ma, which indicated that the latter may have to be revised downward.

Olivine-rich dolerite intrusions are common in the Sierra Baguales, forming huge, laccolite-like sills reaching many tens of meters in thickness, as well as dikes up to 3 m thick (Fig. 3). Field evidence shows that none of these sills penetrates the Santa Cruz Formation, suggesting that their intrusion occurred before the deposition of this unit.

The “Andesitic Lavas of Sierra Baguales” (Muñoz, 1981) are of late Pliocene age and overlie the Santa Cruz Formation, forming prominent cliffs in the high mountains to the north and east of the Río Baguales. These lavas, as well as all the Cretaceous and Miocene successions below, have been intruded by younger dioritic and basaltic dikes with an E-W trend.

In spite of its location close to the fold-and-thrust belt of the Rocas Verdes Basin, the Sierra Baguales area is relatively undeformed, with very gentle folding and faults being almost absent. Our measurements throughout the study area indicate a mean strike and dip of  $303^\circ/10^\circ$ NE.

## 4. Lithostratigraphy and depositional environments

### 4.1. Tres Pasos Formation

This formation is described by Bernhardt (2011) and Macauley and Hubbard (2013) as a continental slope system. In the vicinity of the Río Las Chinas and Cerro Guido the succession consists of decimeter-scale intercalations of fine-grained sandstones, siltstones, and organic-rich shales (Fig. 4A) in occasional fining-upward cycles. The sandstones show lower flow regime horizontal lamination and rare flutes at the base (facies 11 in Table 1). *Rusophycus* trace fossils, probably formed by arthropods, are abundant. This facies is typical of distal turbidites and suggests a continental slope environment. Towards the top of this formation there is a coarsening-upward trend with fine- to very coarse sandstone beds showing high-angle tabular and trough cross-lamination, in which trace fossils of *Rusophycus*, *Palaeophycus* (Fig. 4B), *Cruziana* (Fig. 4C), fish trails or undichnia (Fig. 4D), *Psilonichnus* (Fig. 4E), and *Skolithos* (Fig. 4F) are present. This facies assemblage (mainly facies 10 in Table 1, but elements of facies 9 are also present)

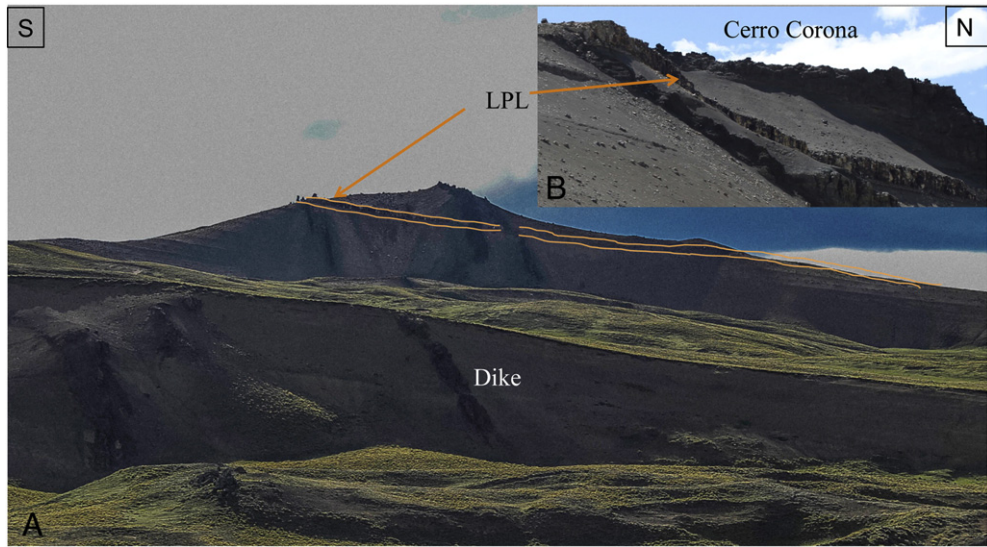


Fig. 3. A) Vertical dike intruding Estancia 25 de Mayo Formation. B) Pyroclastic bed (LPL) in the Estancia 25 de Mayo Formation.

suggests a transition to shallow marine conditions ranging from the shelf or lower shoreface to an upper shoreface with ridges and runnels. There is a thus a gradual transition into the deltaic facies of the Dorotea Formation.

4.2. Dorotea Formation

According to previous authors (Katz, 1963; Riccardi and Rolleri, 1980; Schwartz and Graham, 2015), this formation was deposited in a

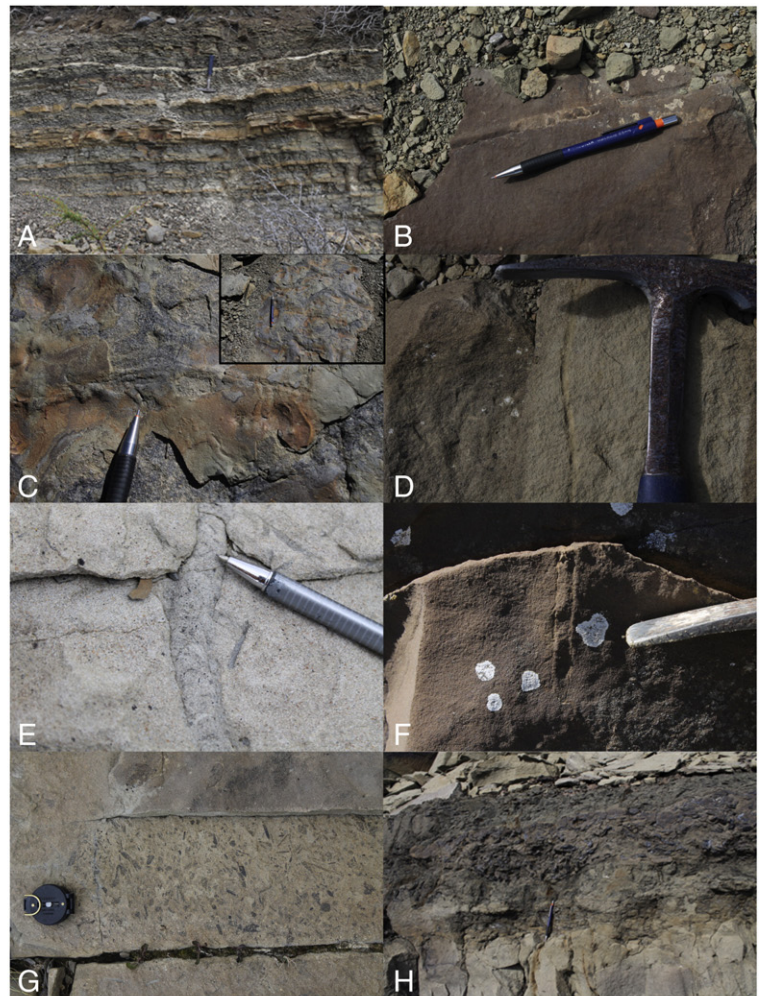
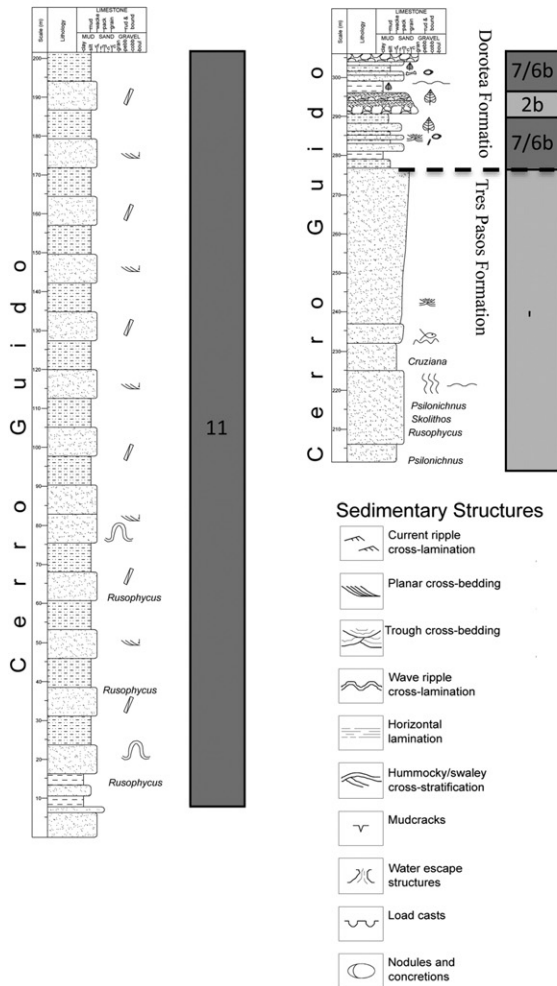


Fig. 4. Measured stratigraphic column of the Tres Pasos and Dorotea Formations in Cerro Guido. A) Turbidites; B) Palaeophycus; C) Cruziana; D) Fish trails (undichnia); E) Oyster bank; F) Wood and leaf fragments; G) *Psilonichnus*; H) *Skolithos*.

**Table 1**  
Depositional facies recognized in the Upper Cretaceous to middle Miocene stratigraphic succession of the Sierra Baguales.

Id	Facies	Formation	General description
1	1a. Braided rivers with abandoned channels. 1b. Braided rivers proximal to ocean.	Santa Cruz, Río Leona. Man Aike	<b>Lithology:</b> Fining- and coarsening-upward, medium- to coarse, greenish sandstones and conglomerates with mud clasts; mudstone and calcareous, very fine-grained sandstone lenses within sandstones. <b>Sedimentary structures:</b> High-angle tabular and trough cross-lamination. <b>Fossils:</b> High content of tree trunks and poorly preserved leaf fragments; shark teeth in 1b.
2	2a. Point bars in meandering rivers. 2b. Point bars in meandering distributary channels.	Río Leona, Santa Cruz. Tres Pasos, Dorotea, Man Aike.	<b>Lithology:</b> Three types of fining-upward cycles: Medium-grained sandstone to nodular mudstone; coarse- and medium-grained sandstone to fine- and very fine-grained sandstone; coarse, clast-supported, monomictic conglomerate to fine conglomerate. Conglomerates contain very fine-grained sandstone lenses. <b>Sedimentary structures:</b> High-angle tabular and trough cross-lamination; upper flow regime parallel lamination; rib-and-furrow structures; current ripple marks in 2a; wave ripples in 2b. <b>Fossils:</b> Bivalves, oysters, shark teeth in 2b, vertebrates, arthropods, tree trunks and leaves in 2a.
3	Levees	Santa Cruz	<b>Lithology:</b> Thin, intercalated beds of siltstone and very fine-grained sandstone.
4	Subaerial flood plains.	Dorotea, Río Leona, Santa Cruz.	<b>Lithology:</b> Multicoloured mudstones with thin, grey to brown shale, reddish siltstone and fine-grained sandstone beds and lenses. <b>Fossils:</b> Wood fragments, leaves, pollen, vertebrates.
5	Overbank swamps.	Río Leona.	<b>Lithology:</b> Sapropelite interbedded with black mudstone. <b>Fossils:</b> Wood fragments and leaves.
6	6a. Crevasse splays on flood plains. 6b. Crevasse splays in interdistributary bays	Río Leona, Santa Cruz. Tres Pasos, Dorotea, Man Aike, Estancia 25 de Mayo.	<b>Lithology:</b> Fine- to medium-grained sandstone; quartz and chert clasts; calcareous sandstone beds with CaCO <sub>3</sub> nodules in 6b. <b>Fossils:</b> Tree trunks, leaves, vertebrate fragments in 6a. Bivalves, gastropods, oysters, shark teeth, leaves, tree trunks, vertebrate fragments in 6b.
7	Estuaries and interdistributary bays.	Dorotea, Man Aike, Estancia 25 de Mayo.	<b>Lithology:</b> Greenish grey mudstones and grey to brown shales with thin interbeds of siltstone and fine-grained sandstone. <b>Fossils:</b> Wood fragments, leaves, bivalves, oysters, shark teeth.
8	8a. Low-sinuosity meandering rivers. 8b. Tidal channels	Santa Cruz. Dorotea, Man Aike.	<b>Lithology:</b> Coarse- to medium-grained sandstones and clast-supported, monomictic conglomerates; beds and lenses have erosional bases; CaCO <sub>3</sub> nodules. <b>Sedimentary structures:</b> Upper flow regime horizontal lamination; high-angle tabular and trough cross-lamination; herringbone cross-lamination in 8b. <b>Fossils:</b> Burnt wood fragments in 8a. Burnt wood fragments, shark teeth in 8b. <b>Trace fossils:</b> <i>Skolithos</i> in 8b.
9	Upper shoreface with shoals, ridges and runnels, occasional distributary mouth bars.	Tres Pasos, Dorotea, Man Aike, Estancia 25 de Mayo.	<b>Lithology:</b> Coarse- to very coarse-grained sandstones and conglomerates in coarsening-upward cycles; sandstones contain fine-grained sandstone lenses. <b>Sedimentary structures:</b> High-angle tabular and trough cross-lamination. <b>Fossils:</b> Wood and leaf fragments, <i>Turritella</i> , gastropods, oysters, crabs.
10	Shelf to lower shoreface	Estancia 25 de Mayo.	<b>Lithology:</b> Fine- to medium-grained sandstone interbedded with shale; CaCO <sub>3</sub> nodules and concretions. <b>Sedimentary structures:</b> Lower flow regime horizontal lamination. <b>Fossils:</b> Gastropods, brachiopods, crabs, leaves.
11	Continental slope, turbidity currents	Tres Pasos.	<b>Lithology:</b> Medium- to fine-grained sheet sandstones interbedded with thin, organic-rich shales; occasional fining-upward cycles. <b>Sedimentary structures:</b> Lower flow regime horizontal lamination, rare flute marks. <b>Ichnofossils:</b> <i>Rusophycus</i> .

transitional, shallow marine to deltaic environment. It contains invertebrate, vertebrate, insect and plant fossils, while traces of *Skolithos* and *Thalassinoides* are common.

In the Cerro Guido section (Fig. 4, left) this formation concordantly overlies the Tres Pasos Formation, consisting of greenish grey mudstones and grey to brown shales with thin interbeds of siltstone and fine-grained sandstone (facies 7 in Table 1). Fining-upward conglomerates filling channels also occur (facies 2), while fossils are represented by wood and leaf fragments (Fig. 4G), bivalves, shark teeth and oyster accumulations (Fig. 4H). This section is interpreted as representing estuaries or interdistributary bays with oyster banks.

Five depositional facies were recognized in the profile of the Dorotea Formation measured at Las Tetas de las Chinas (Fig. 5). The first (facies 4; Table 1) consists of up to 40 m of reddish to greenish and grey mudstones with bed thicknesses between 10 and 30 cm, intercalated with cm-scale horizons of grey to brown shale. Thin lenses of fine- to medium-grained sandstone are also present. These deposits contain fossil wood and leaves, pollen, and vertebrate fragments, being interpreted as representing overbank flood plains with small channels and shallow ponds.

The second (facies 2; Table 1) is represented by 2–5 m thick, grey, medium- to coarse-grained sandstones with erosional bases, separated by mudstones. The sandstones display trough and high-angle planar

cross-lamination as well as upper flow regime parallel lamination (Fig. 5K), rib-and-furrow structures (Fig. 5L), and wave ripples (Fig. 5G). Trace fossils are represented by *Arenicolites* (Fig. 5C, D) and arthropod trails (Fig. 5E, F). Meter-scale lenses of brown, very coarse-grained sandstones with high-angle planar cross-lamination are also present. This facies reflects low-sinuosity distributary channels with lunate and straight-crested bars under the influence of wave action.

The third (facies 6; Table 1) is up to 5 m thick, being composed of brown, calcareous, fine- to medium-grained sandstones with chert and quartz clasts as well as carbonate nodules. Bivalves and gastropods are present. They are interpreted as crevasse splay deposits partially filling interdistributary bays, as they are interbedded with facies 7.

The fourth (facies 9; Table 1) consists of up to 5 m thick cycles of coarse to very coarse sandstones grading upward into conglomerates with chert and quartz clasts reaching 14 cm in diameter. The sandstones display trough- and high-angle planar cross-lamination (Fig. 5J) and contain fine-grained sandstone lenses. Fossil leaves and wood fragments are present. These characteristics suggest prograding upper shoreface deposits with ridges and runnels, or possibly distributary mouth bars.

The fifth association (facies 2b; Table 1), displays three types of fining-upward cycles: up to 8 m of medium sandstone grading into mudstone with calcareous nodules; medium sandstone grading into fine

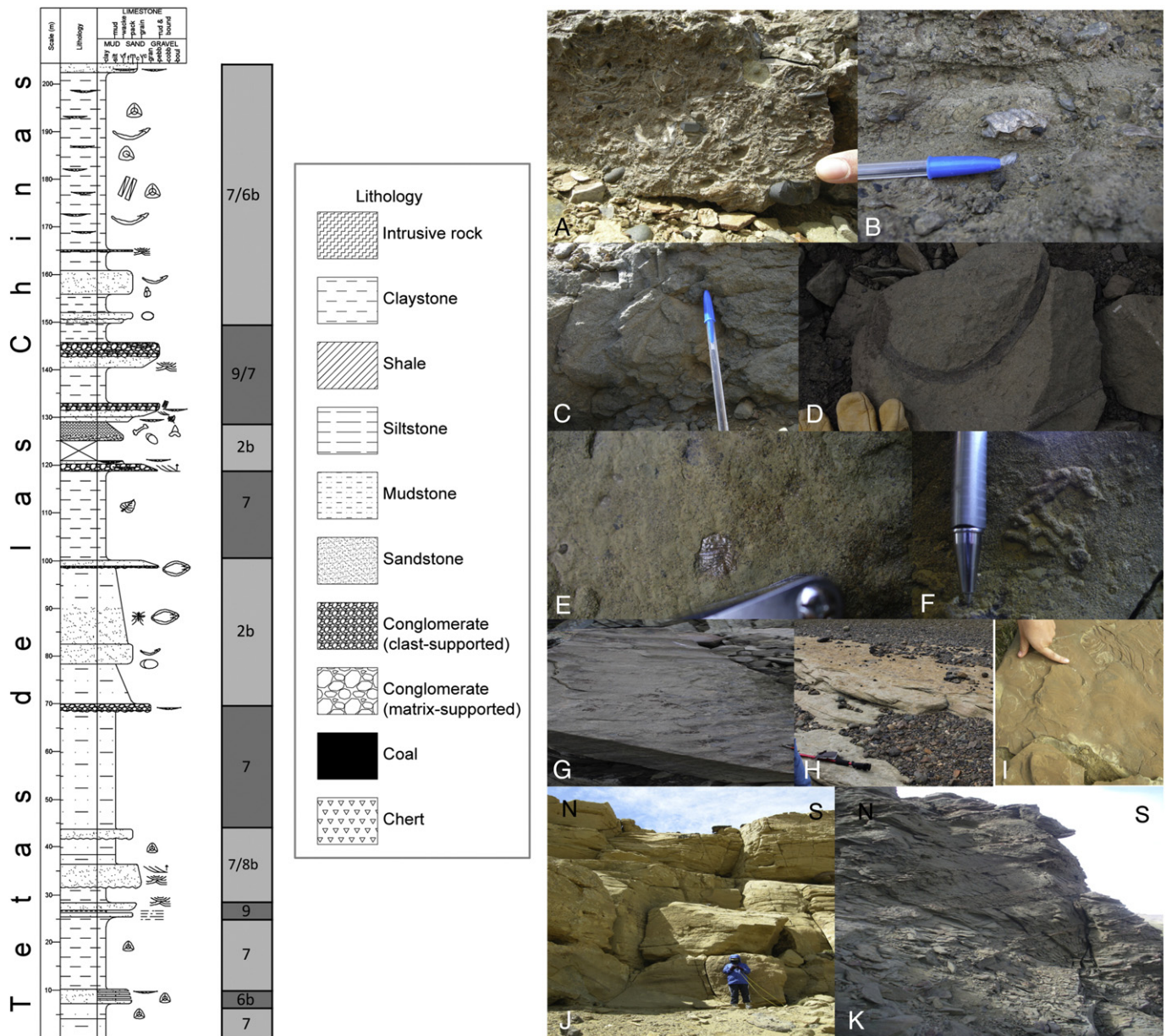


Fig. 5. Measured stratigraphic column of Dorotea Formation at Las Tetas de las Chinas. A) Bivalves; B) Oysters; C and D) *Arenicolites*; E) Arthropod; F) Arthropod trails; G) Wave ripples; H) Trough cross-lamination; I) Rib-and-furrow structures; J) High-angle tabular and trough cross-lamination; K) upper flow regime horizontal lamination.

sandstone over a total thickness of 20 m; and up to 2 m thick cycles of coarse conglomerate grading into monomictic, clast-supported conglomerates with rounded chert clasts reaching 10 cm in diameter. In the latter cycles, the conglomerates show high-angle cross-bedding and contain fine-grained sandstone lenses. Fossils include shark teeth, vertebrate fragments, insects, bivalves and oysters. This facies is interpreted as representing meandering distributary channels directly connected to the open sea.

The characteristics described above therefore indicate a shallow marine, deltaic environment for the Dorotea Formation, in which subaerial delta plains with low to higher sinuosity distributary channels and overbank sediments graded laterally into interdistributary bays with crevasse splays. Distributary mouth bars developed on the upper shoreface where the channels entered the underwater platform. This interpretation coincides with those of Gutiérrez et al. (2013), González (2015), and Schwartz and Graham (2015), based on other profiles measured in the Dorotea Formation.

#### 4.3. Man Aike Formation

The middle part of the Man Aike Formation was deposited in a mainly wave-dominated estuary, but with extensive tidal flats (Le Roux et al., 2010). A 50 m thick profile was measured in the Chorrillo Jabón sector and 40 m in the Las Tetas de las Chinas sector (Fig. 6). The first is complementary to the top of the Man Aike Formation measured by and referred to as the Río Bagaules Formation by Le Roux et al. (2010), whereas the second corresponds to the base of this column. In the measured base and top of the Man Aike Formation, three different facies were recognized, all containing shark teeth. The first (facies 1a; Table 1) consists of medium to coarse sandstone with both coarsening- and fining-upward trends, displaying high-angle tabular and trough cross-lamination and decimeter-scale mudstone lenses. Poorly preserved wood and leaf fragments are present. It is interpreted as representing braided streams in a general estuary environment. The presence of shark teeth indicates proximity to the ocean. The second

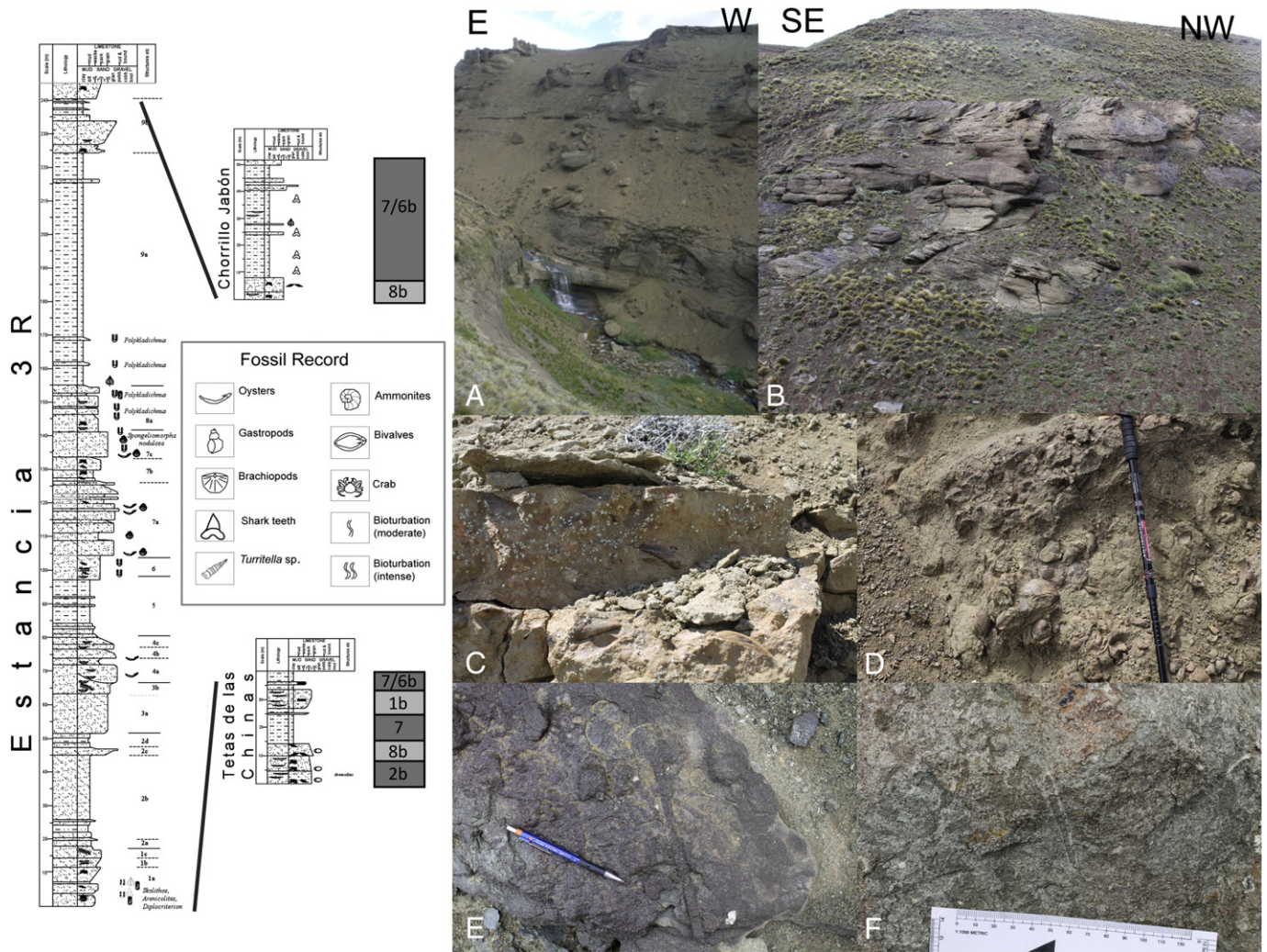


Fig. 6. Measured stratigraphic columns of Man Aike Formation at Las Tetas de las Chinas and Chorillo Jabón. A) Outcrop of Man Aike Formation at Chorillo Jabón; B) Herringbone cross-lamination; C) Bivalves; D) Gastropods; E) and F) *Skolithos*.

facies (facies 7; Table 1) is dominated by mudrocks interbedded with fine- to medium-grained sandstone beds and lenses. Bivalves and gastropods are present (Fig. 6C, D) in addition to shark teeth. This facies is considered to reflect an estuary. The third facies (facies 8b; Table 1) is represented by medium- to coarse-grained sandstones with erosional bases showing herringbone (Fig. 6B) and trough cross-lamination. Trace fossils are represented by *Skolithos* (Fig. 6E, F). This facies reflects tidal channels subjected to ebb and flow. The association is thus typical of tide-dominated estuaries, which is consistent with the interpretation of Le Roux et al. (2010).

4.4. Río Leona Formation

The Río Leona Formation was deposited in a fluvial environment characterized by meandering and anastomosing rivers with wide overbank flood plains (Marensi et al., 2000, 2005).

A composite section of the Río Leona Formation was measured at Chorillo Jabón and Las Murallas, respectively (Fig. 7), in which 6 depositional facies were identified. The first (facies 4; Table 1) consists of brown to greenish, massive mudstones interbedded with siltstones and very fine-grained, grey to dark grey sandstones. Its thickness varies between 5 and 20 m. Fossil tree trunks and leaves were also recorded. This facies is attributed to a subaerial, overbank environment.

Buff, fine to medium-grained sandstones up to 1 m thick intercalated with buff to brown mudstones compose the second facies (facies 6a,

Table 1). Fossil roots, trunks and leaves (Fig. 7C–F) are present, indicating a subaerial environment. This facies reflects crevasse splays in an overbank environment.

The third association (facies 2a, Table 1) is composed of coarse- to fine-grained sandstones forming 2–5 m thick, fining-upward cycles. Current ripple marks occur at the top of some cycles, with fossil wood fragments and leaves also present. These are interpreted as point bars in meandering channels.

The fourth facies (facies 1a; Table 1) displays greenish, medium- to coarse-grained sandstones with intraformational mud-clast conglomerates. Both coarsening- and fining-upward cycles are present. Sedimentary structures include trough and high-angle tabular cross-lamination. Mudstone lenses with erosional basal and upper contacts and some calcareous sandstone lenses were also recorded. There are abundant, but poorly preserved fossil tree trunks and leaves. This facies represents braided streams with abandoned channels.

Facies 5 (Table 1) consists of sapropelite interbedded with black mudstones, indicating a high organic content that coincides with the presence of abundant fossil wood fragments and leaves. It is interpreted as representing swampy, reducing conditions within an overbank environment.

The overall sedimentological characteristics of the Río Leona Formation thus suggest a coastal plain with meandering and locally braided channel systems. Flood plain swamps created reducing conditions in which wood and leaf fragments were well preserved. This



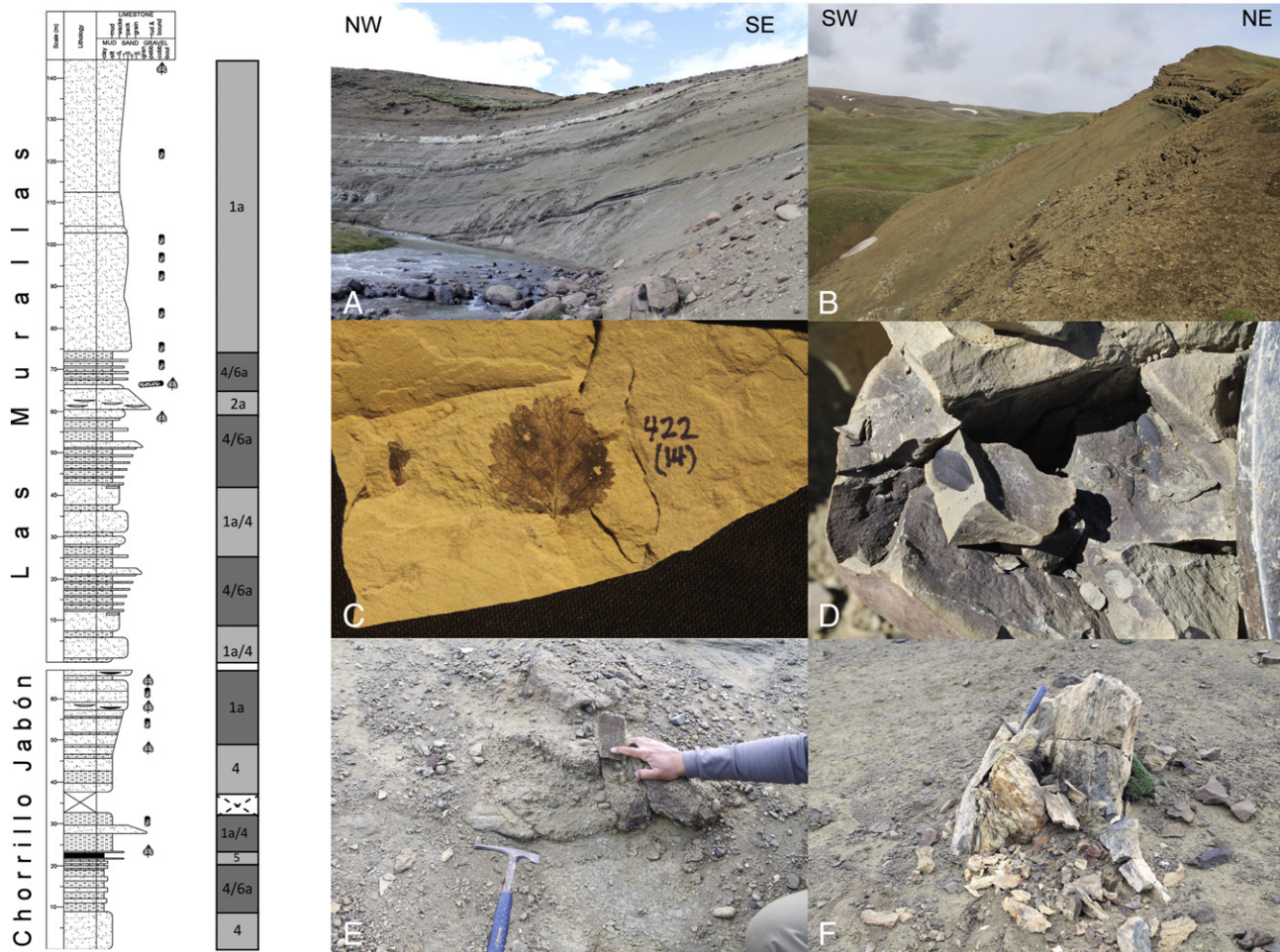


Fig. 7. Measured stratigraphic columns of Río Leona Formation at Las Murallas and Chorrillo Jabón. A) and B) Outcrops of Río Leona Formation at Las Murallas and Chorrillo Jabón; C) and D) Well preserved fossil leaves; E) Wood fragment in conglomerate; F) tree trunk in life position.

interpretation of the Río Leona Formation is consistent with previous studies of this formation in Argentina and Chile (Malumián, 1990; Marensi et al., 2000, 2002, 2005; Le Roux et al., 2010; Malumián and Nañez, 2011; Cuitiño et al., 2013).

#### 4.5. Estancia 25 de Mayo Formation

Two facies were recognized in this formation. The first (facies 10, Table 1) consists of thin (1–2 m), sheet-like beds of greenish, fine- to medium-grained, calcareous sandstones. These are intercalated with ochre to brown, calcareous shales, also between 1 and 2 m thick, in which cm-scale, calcareous nodules and fossiliferous concretions are present. Among the fossils are gastropods and crabs, as well as brachiopods and leaves. This facies represents a lower shoreface environment.

The second facies (facies 9; Table 1) is composed of massive, medium- to coarse-grained, calcareous sandstones showing ochre to greenish colours, calcareous nodules and concretions containing gastropods (including *Turritella*), crabs (Fig. 9B), articulated brachiopods (Fig. 8B), and oysters (Fig. 8F). The presence of *Turritella* and oysters suggests a nearshore environment in the vicinity of river mouths, so that this facies is interpreted as representing sandy shoals in an upper shoreface environment.

#### 4.6. Santa Cruz Formation

This formation was deposited in meandering rivers on a flood plain with local small lakes. No new stratigraphic profiles were measured in

the Santa Cruz Formation, as this had already been done by the present authors in a previous publication (Bostelmann et al., 2013). The facies recognized in that study (Morro Bayo section; Fig. 9A) included 2–10 m thick units of multicoloured mudstones with abundant vegetal remains, showing metric-scale, reddish siltstone lenses in the thicker units. Vertebrate fossils (Fig. 9B) and pollen are abundant, with occasional insect traces (Fig. 9D). This association (facies 4; Table 1) represents overbank flood plain deposits. Fine- to medium-grained sandstones reflecting crevasse splays (facies 6a; Table 1) are between 1 and 1.5 m thick and interbedded with the mudstone. Meandering channels with point bar deposits (facies 2a; Table 1) are represented by 2–5 m thick, fining-upward, coarse- to fine-grained sandstone with epsilon (Fig. 9F), high-angle tabular (Figs. 9C, 10) and trough cross-lamination (Fig. 9E, H), whereas levees (facies 3; Table 1) are indicated by thin beds (less than 1 m) of siltstone intercalated with very fine sandstone. Somewhat straighter channels (facies 8a; Table 1) are represented by clast-supported, monomictic conglomerates showing erosional basal contacts and trough cross-bedding. Burnt wood fragments are also present. These characteristics indicate a fluvial system dominated by meandering streams, with local minor braided systems.

## 5. Palaeocurrent directions

### 5.1. Tres Pasos Formation

Previous palaeocurrent studies in the Cerro Toro and lower parts of the Tres Pasos Formation indicated a consistent southward-directed

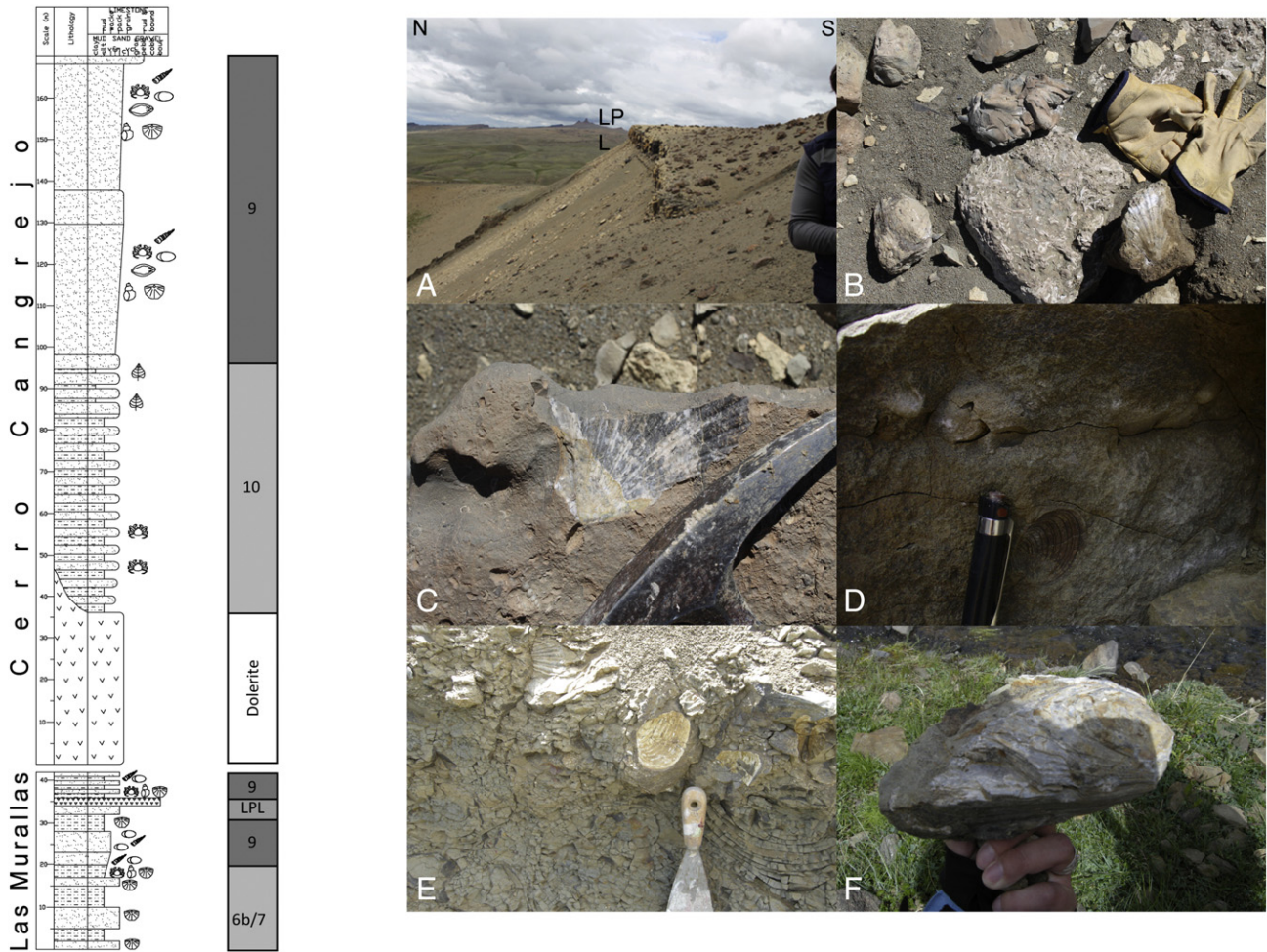


**Fig. 8.** Measured stratigraphic columns of Estancia 25 de Mayo Formation at Las Murallas and Cerro Cangrejo. A) Outcrop of Estancia 25 de Mayo Formation and LPL bed at Las Murallas. B) Gastropods, *Turritella* and crabs; C)–E) Brachiopods; F) Oysters.

dispersal pattern (Scott, 1966; Fildani and Hessler, 2005; Crane and Lowe, 2008; Hubbard et al., 2008, 2010; Bernhardt et al., 2008, 2011; Jobe et al., 2010; Romans et al., 2010). Palaeocurrent directions in the Tres Pasos Formation were mainly derived from the inclination direction of slope clinoforms, lateral facies changes indicating southward progradation, and sole structures such as tool and flute marks. Measured directions vary between 160 and 180° (Hubbard et al., 2010). Our identification of shelf to lower shoreface facies in the upper part of the Tres Pasos Formation in the Sierra Baguales concurs with these studies, in that it represents a more proximal, shallow marine environment in comparison with the continental slope facies identified further south by Bernhardt (2011) and Macauley and Hubbard (2013). The source area was therefore located mainly to the north.

5.2. Dorotea Formation

In the Dorotea Formation (Campanian to Maastrichtian), the 55 measured palaeocurrent directions in the Sierra Baguales are towards the west with a range between southwest and northwest (Fig. 10A). This is consistent with the type of depositional environment, being a tide-dominated delta. However, the vector mean is 269° with a vector magnitude of 84%, suggesting that the source area was situated mainly to the east. Forty-one palaeocurrents measured by us further south at Cerro Castillo (Fig. 1) gave a vector mean of 241° with a vector magnitude of 32%.

5.3. Man Aike Formation

Only 9 measurements were taken in the Man Aike Formation (Lutetian to Bartonian) in the Sierra Baguales, which display two trends. The main trend is towards the west-northwest and the second towards the east (Fig. 10B). The vector mean is 295° with a magnitude of 43%. This coincides with an estuary environment (Le Roux et al., 2010) subjected to ebb and flow tides as shown by herringbone cross-lamination. We also measured 32 palaeocurrent directions in the time-equivalent Loreto Formation west of Punta Arenas (Fig. 1), yielding a vector mean of 291° with a vector magnitude of 18%. This set also shows two modes, one with a vector mean of 289° (n = 19) and another (n = 13) with a vector mean of 104°.

5.4. Río Leona Formation

The Río Leona Formation (Rupelian) yielded 18 measurements with three preferential directions towards the south, northwest and northeast, respectively (Fig. 10C). The last concentrates the majority of readings, with a vector mean of 56° and a magnitude of 63%.

5.5. Estancia 25 de Mayo Formation

In the Estancia 25 de Mayo Formation (early Burdigalian), 37 palaeocurrent directions were recorded, which are dominated by two

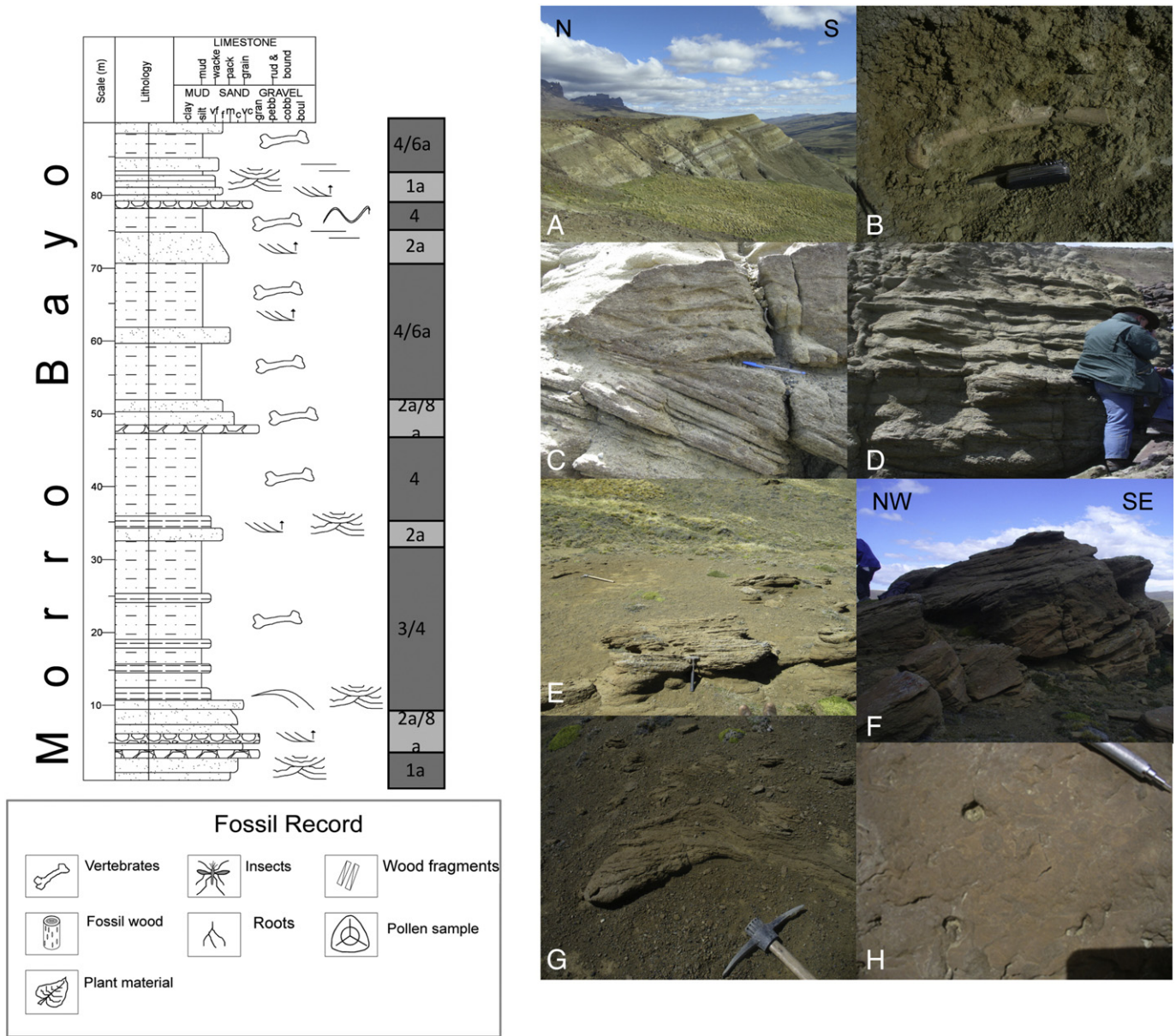


**Fig. 9.** Measured stratigraphic column of Santa Cruz Formation in Morro Bayo (after Bostelmann et al., 2013). A) Outcrops of the Santa Cruz Formation; B) Vertebrate bone; C–D) Tabular cross-lamination; E–F) Trough cross-lamination; G) Epsilon cross lamination; H) Insect trails.

trends, namely north and southeast (Cuitiño, 2011). The vector mean is  $55^\circ$  with a magnitude of 36% (Fig. 10D).

### 5.6. Santa Cruz Formation

In the Santa Cruz Formation (late Burdigalian), 73 palaeocurrents were recorded with a vector mean of  $65^\circ$  and a magnitude of 83% (Fig. 10E).

### 5.7. Summary of palaeocurrent directions

Our measured palaeocurrent directions and vector magnitudes in the Sierra Baguales indicate that they were directed mainly towards the west ( $269^\circ$ ) between the Cenomanian and Maastrichtian, varying from southwest to west-northwest. This is consistent with 86 palaeocurrent directions measured by us in the Thanetian ( $57.6 \pm 1$  Ma; Sánchez et al., 2010) “Cabo Nariz Beds” on Tierra del Fuego in the southern part of the Magallanes-Austral Basin, which gave a vector mean of  $300^\circ$ . The north-westerly trend was maintained at least until the Bartonian-Priabonian,

when a vector mean of  $295^\circ$  was recorded in the Man Aike Formation. However, during the Rupelian and early Chattian an abrupt swing to the northeast ( $055^\circ$ ) occurred, shifting to east-northeast ( $065^\circ$ ) during the Burdigalian. Additionally, the data show a decrease in the vector magnitude between the Río Leona and Estancia 25 de Mayo Formations, changing from 63% to 36%. This decrease coincides with a change in the depositional environment, passing from meandering and braided rivers in the Río Leona Formation to a shoreface environment in the Estancia 25 de Mayo Formation. After deposition of the latter, there was an increase in the vector magnitude from 36% to 86%, which coincides with a new change in depositional environment from shoreface to continental, fluvial conditions in the Santa Cruz Formation.

## 6. Detrital zircons and radiometric ages

### 6.1. Tres Pasos Formation

The Tres Pasos Formation was dated by Bernhardt (2011) in the Silla Syncline to the south of the Sierra Baguales between  $89.5 \pm 1.9$

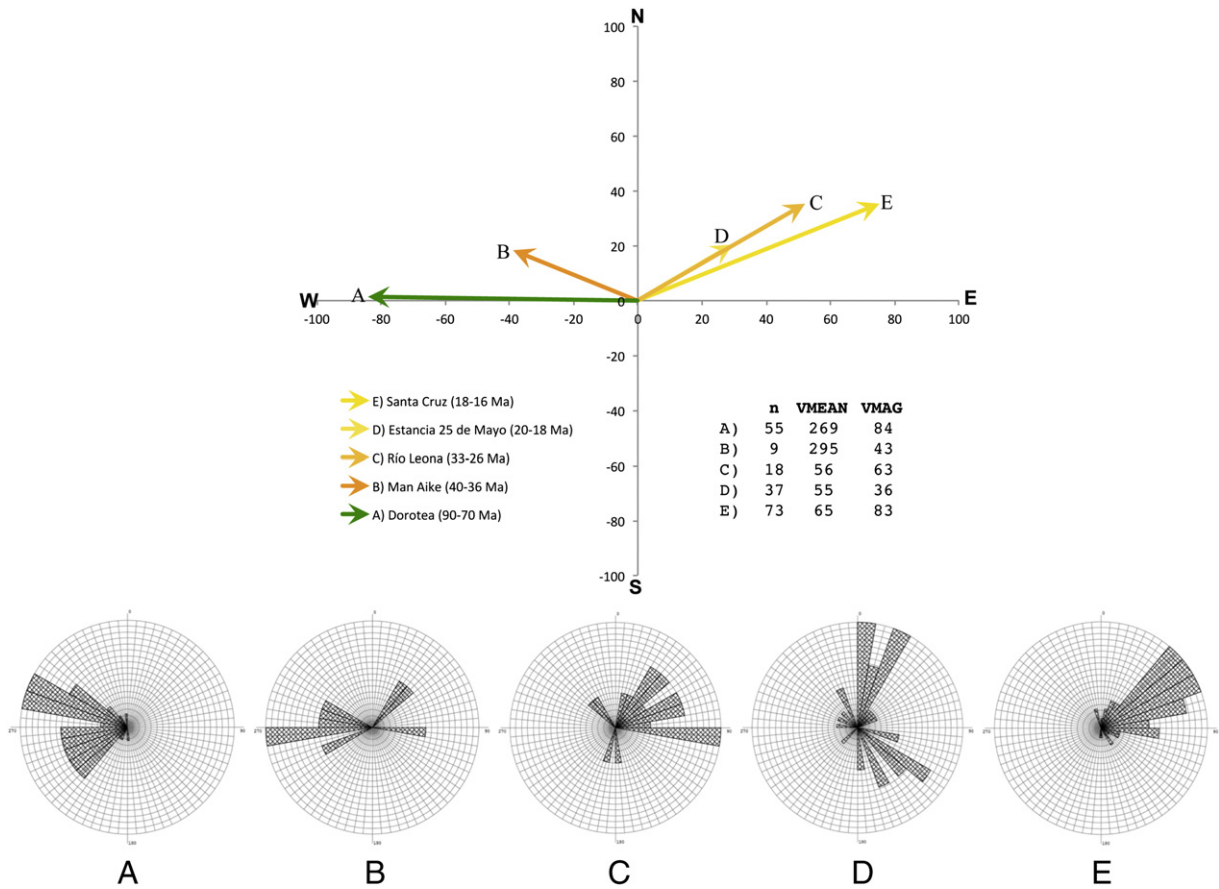


**Fig. 10.** Rose diagrams of palaeocurrent directions in the different formations of the Sierra Baguales. A) Dorotea Formation; B) Man Aike Formation; C) Estancia 25 de Mayo Formation; D) Río Leona Formation; E) Santa Cruz Formation.

(Turonian) and  $81.7 \pm 1.7$  Ma (Campanian), using Sr isotopes as well as detrital and volcanic zircons. The last age is supported by the presence of *Hoplitoplacenticeras plasticus* and *H. semicostatus* ammonites at Cerro Cazador (Paulcke, 1907). Her sample SdT-Wc, collected from just north of Lago del Toro about 40 km south of the Sierra Baguales, contained 2 detrital zircons with ages exceeding 1000 Ma, 13 with ages between 672 and 251 Ma, and 16 between 155 and 93 Ma. These are here assigned to groups I, IIe and IIIe, respectively.

6.2. Dorotea Formation

Sample Zr-PTO-123 (Fig. 11, top) was collected from the base of the Dorotea Formation at Cerro Guido. The results of detrital zircon dating show 5 populations with ages ranging from 636–480 Ma, 423–310 Ma, 270–171 Ma, 151–139 Ma, and finally 127–84 Ma. The latter population has a mean maximum depositional age of  $92.78 \pm 0.76$  Ma. However, the youngest zircon yielded a date of  $83.9 \pm 2.6$  Ma (late Santonian). Two further samples, Zr-FB-1 (Fig. 11, bottom) and Zr-FB-2 (Fig. 12, top), were collected in the sector Las Tetras de las Chinas, from the middle and upper part of the Dorotea Formation, respectively. Detrital zircon dating of sample Zr-FB-1 shows 3 populations: the first with ages ranging from 578 to 390 Ma, the second with dates between 158 and 123 Ma, and the third group of 31 zircons varying between 112 and 71 Ma. The mean maximum depositional age is  $95.1 \pm 1.5$  Ma (Cenomanian). Similarly, 3 populations were also identified in sample Zr-FB-2, the first between 512 and 406 Ma, the second from 380 to 268 Ma, and the final group ranging from 152 to 72 Ma. In this case the mean maximum depositional age is  $93.7 \pm 1.2$  Ma. However, two zircons in sample Zr-FB-1 have ages of  $74.9 \pm 2.1$  and  $71.0 \pm 1.2$  Ma (Campanian), respectively, whereas one zircon in sample Zr-FB-2 has an age of  $71.7 \pm 1.2$  Ma. The latter dates are supported by the

presence of *Gunnarites* sp., *Pachydiscus* aff. *gollevilensis*, and *Pachydiscus cazadoriana* in the Dorotea Formation in the vicinity of Las Tetras de las Chinas (González, 2015). The first two fossils are of Maastrichtian age (Martínez-Pardo, 1965), while the last is from the Campanian-Maastrichtian (Otero et al., 2009). A vertebrate fragment of *Aristonectes* sp. (Plesiosauria, Elasmosauridae) reported by Otero et al. (2015) at the same locality also indicates a late Maastrichtian age, while the presence of *Hoplitoplacenticeras* ammonite species at Cerro Cazador suggests a Campanian age for the basal part of the Dorotea Formation (Macellari et al., 1989). In addition, in the Cordillera Chica and Sierra Dorotea, where the Dorotea Formation also crops out, maximum depositional ages between 72 Ma and 67 Ma were obtained from detrital zircons (Hervé et al., 2004; Fosdick et al., 2015a, 2015b). Therefore, although the possible age of the Dorotea Formation ranges from the late Cenomanian to Maastrichtian (Late Cretaceous), the youngest zircons as well as ammonite fossils indicate a Campanian-Maastrichtian age.

Taking account of the overlapping ages of the populations from different samples, two general groups can be distinguished, namely IIe, between 636 and 171 Ma, and IIIe, between 158 and 67 Ma.

6.3. Man Aike Formation

A sample from the top of this formation, Zr-PTO-77 (Fig. 12, bottom), from the locality of Chorrillo Jabón shows 3 zircon age populations ranging from 550–450 Ma, 143 Ma–72 Ma, and 49 Ma–35 Ma, respectively. The first two populations therefore correspond to the broad groups IIe and IIIe defined in the Dorotea Formation, while the third, here referred to as IV, is younger. The maximum depositional age of a population with 39 zircons is  $40.30 \pm 0.47$  Ma. A mean maximum zircon age of  $40.48 \pm 0.37$  Ma was also reported by Le Roux (2012a), Bostelmann et al. (2012)

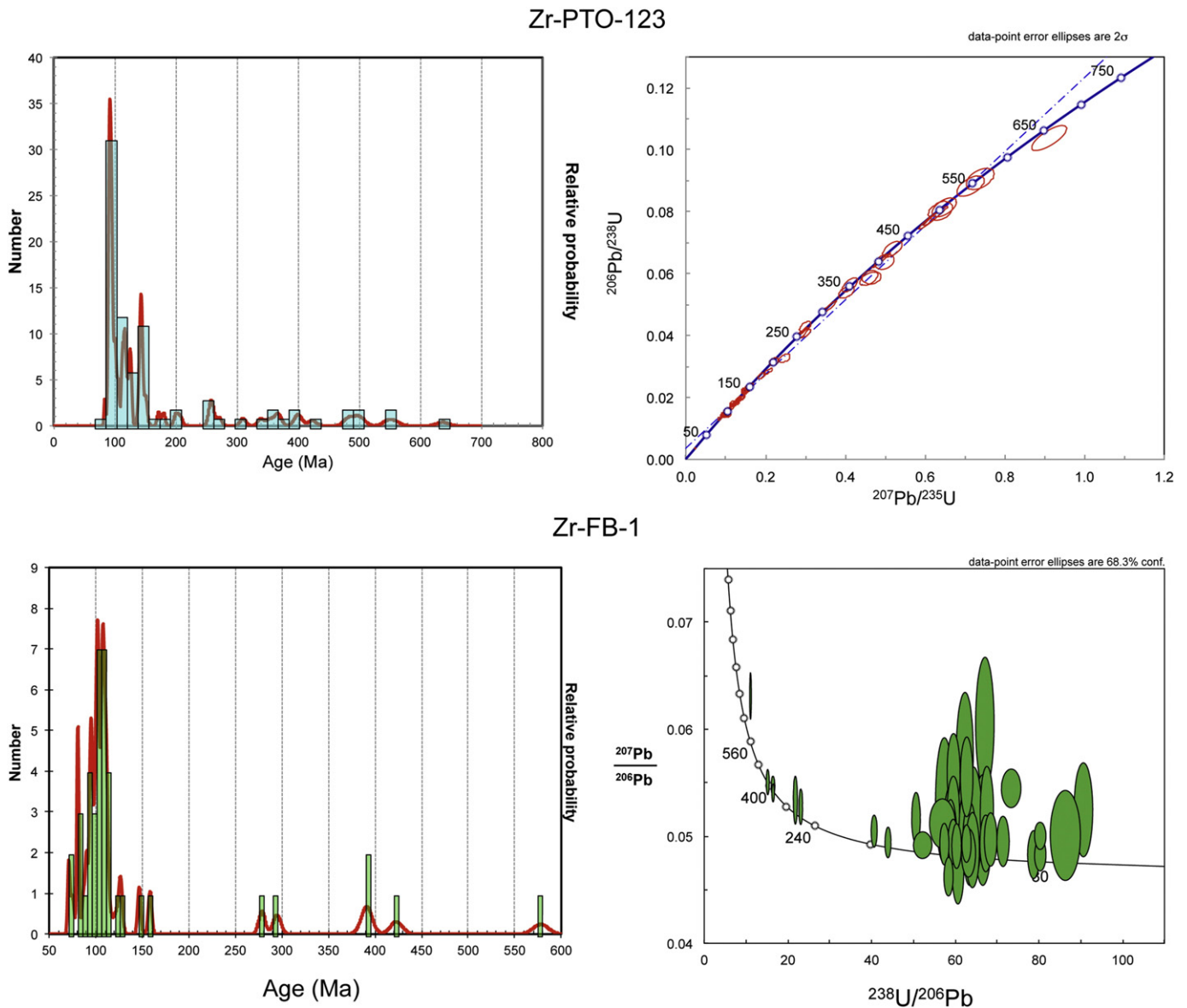


Fig. 11. U-Pb detrital zircon ages in sample PTO-123 and ZR-FB-1 from the Dorotea Formation.

and Otero et al. (2013), so that a latest Lutetian to Bartonian (middle Eocene) age can be accepted. Although Le Roux (2012a) and Bostelmann et al. (2012) never published the details of this sample collected from the top of the Man Aike Formation in a stratigraphic profile measured on Estancia 3R (Le Roux et al., 2010), the results are consistent with those of sample Zr-PTO-77.

#### 6.4. Río Leona Formation

Sample Zr-PTO-81 (Fig. 13, top) was collected from Chorrillo Jabón, being a feldspathic wacke located at the base of the Río Leona Formation. The zircons show three populations, the first with ages exceeding 120 Ma and the second dating between 100 Ma and 76 Ma. Both populations belong to group IIIw. The third population has ages between 43 Ma and 30.8 Ma, therefore belonging to group IV, with a mean calculated age of  $35.33 \pm 0.57$  Ma. Again, the 17 youngest zircons have ages less than 35 Ma, forming a sub-population with a mean of  $33.0 \pm 2.8$  Ma, which is thus taken as the maximum depositional age.

Sample Zr-BAG-25 (Fig. 13, bottom) was collected from Chorrillo las Flores (Fig. 1B) by Ugalde (2014) in the stratotype section of the former Las Flores Formation of Cecioni (1957), which was redefined by the first

author as being from the top of the Man Aike Formation. The sample is a feldspathic wacke. The detrital zircon dates show 4 populations, the first with ages exceeding 117 Ma, the second with dates between 108 Ma and 93 Ma, and the third with ages ranging from 80 Ma to 68 Ma. These therefore correspond to group IIIw. The final population lies between 46 Ma and 30 Ma, extending the lower range of group IV by 5 Ma. Although the calculated maximum depositional age for the latter population is  $37.0 \pm 0.27$  Ma (Priabonian), the 16 youngest zircons are all less than 35 Ma old. Taking these as a sub-population, they yield a mean age of  $32.83 \pm 0.65$  Ma, which is here taken to represent the maximum depositional age, i.e. Rupelian (early Oligocene). The presence of fossil leaves of Nothofagaceae, fossil wood belonging to the Araucariaceae, and palynological records of pollen, spores and organic material of plant origin, deposited in an environment of tidal bars and flats (Ugalde, 2014), suggests that this section in fact corresponds to the base of the Río Leona Formation (see Fig. 13, modified from Ugalde, 2014).

The lithological similarity between samples Zr-PTO-81 and Zr-BAG-25, together with the fact that they show very similar zircon population groups and have coinciding maximum depositional ages of 33 Ma, supports the idea that both are from the base of the Río Leona Formation, which is therefore considered to be of Rupelian age.

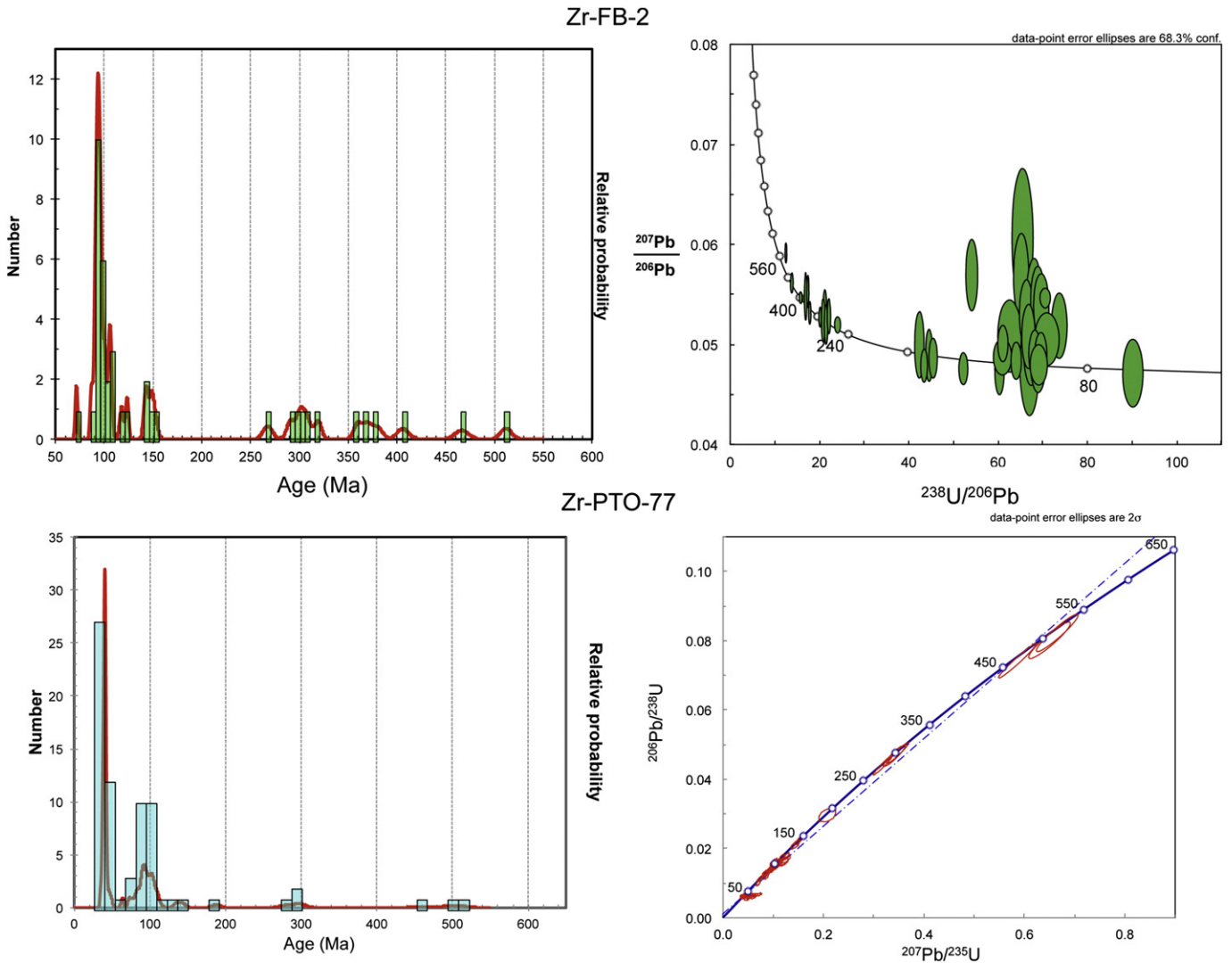


Fig. 12. U-Pb detrital zircon ages in sample Zr-FB-2 from the Dorotea Formation and U-Pb detrital zircon ages in sample Zr-PTO-77 from the Man Aike Formation.

6.5. Estancia 25 de Mayo Formation

It was not possible to date the Estancia 25 de Mayo Formation using detrital zircons in Sierra Baguales. Nevertheless, in the middle part of the stratigraphic section measured in the Alto Río Bandurrias sector, a 2 m-thick pyroclastic bed with a rhyodacitic composition was identified. This pyroclastic event was also recorded in the Quien Sabe Member of the Lago Argentino sector, where it was referred to as “LPL” by Cuitiño et al. (2012), and yielded a zircon U-Pb age of  $19.14 \pm 0.5$ . Cuitiño et al. (2015) subsequently dated the stratigraphically equivalent El Chacay Formation in the northern Magallanes-Austral Basin at 20.3–18.1 Ma using strontium isotopes. The Estancia 25 de Mayo Formation is therefore of early Burdigalian age.

6.6. Santa Cruz Formation

Two samples were dated from this formation by Bostelmann et al. (2013) using the SHRIMP U-Pb method. Sample Zr-LF-002 (Fig. 14), located stratigraphically 65 m below Zr-LF-001, yielded 70 zircons. The oldest population showed ages exceeding 1000 Ma, here classified into group I. The second ranged from 700 Ma to 500 Ma, in this paper being considered as part of group IIw because palaeocurrents indicate a source to the southwest instead of the east. The third population,

with an age range between 450 Ma and 250 Ma, and the fourth showing ages clustered around 200 Ma, would also form part of group IIw. The fifth population, with ages of 154 Ma – 130 Ma, together with the sixth between 92 Ma and 88 Ma, would belong to group IIIw, distinguished from group IIIe because palaeocurrents indicate a different source area. No younger zircons were present (Fig. 14).

Sample Zr-LF-001 (Fig. 15) was collected from near the top of the exposed Santa Cruz Formation. It contained a total of 70 zircons, of which the oldest 42 could be grouped into 6 populations. The first group has ages between 2927 Ma and 1656 Ma and is here classified into group I. The second population lies between 695 Ma and 560 Ma, the third between 397 Ma and 303 Ma, and the fourth between 299 Ma and 270 Ma, all belonging to group IIw. The fifth population consists of 4 zircons ranging in age between 153 Ma and 142 Ma, and the sixth has 18 zircons dating from 108 Ma to 79 Ma. Both populations belong to group IIIw. For the youngest population of 28 zircons, all falling in group V (with ages less than 25 Ma), Bostelmann et al. (2013) reported a mean calculated age of  $18.23 \pm 0.22$  Ma. However, a new interpretation of these data suggests that the maximum depositional age of the Santa Cruz Formation in the Última Esperanza Province is in fact  $16.8 \pm 0.22$  Ma (late Burdigalian), which is the mean age of a subpopulation of the 8 youngest zircons.

Except for the absence of zircons younger than 25 Ma from sample Zr-LF-001, there is a clear similarity between the population groups of

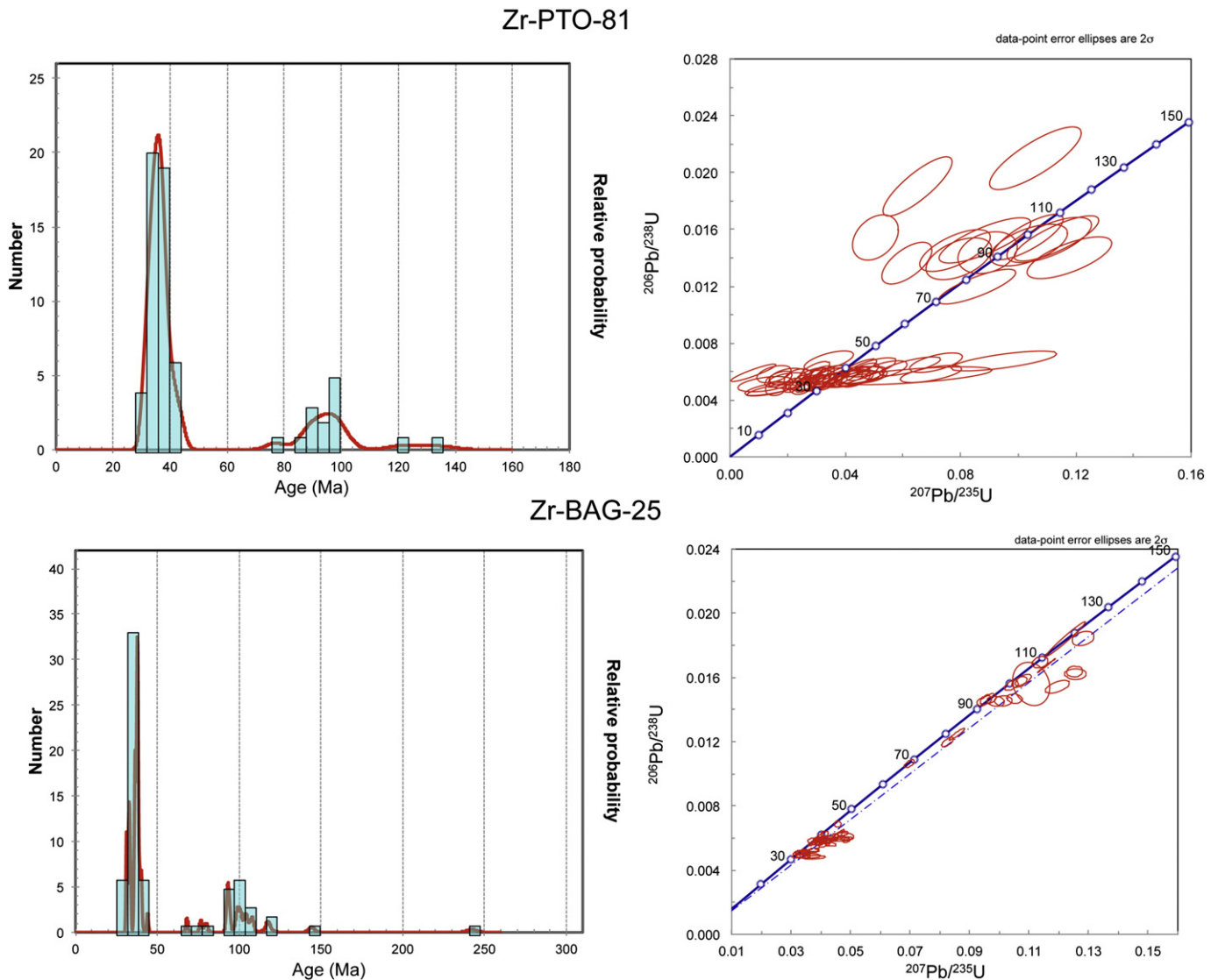


Fig. 13. U-Pb detrital zircon ages in sample Zr-PTO-81 from the Río Leona Formation and U-Pb detrital zircon ages in sample Zr-Bag-25 from the Río Leona Formation (after Ugalde, 2014).

samples Zr-LF-001 and Zr-LF-002, suggesting that the source of the Santa Cruz Formation did not change, but that the younger plutons had either not been exhumed when the base of the formation was being deposited or were not specifically eroded by the rivers delivering detritus to the basin.

## 7. Zircon provenance areas

Romans et al. (2010) summarized the available evidence from detrital zircon ages that indicate potential source areas for the Late Cretaceous deposits in the Magallanes-Austral Basin, based mostly on the work of Pankhurst et al. (2000), Hervé and Fanning (2003) and Hervé et al. (2007). According to the latter authors, detrital zircons older than 168 Ma were derived from metasediments of the Eastern Andean Metamorphic Complex and the Duke de York Complex, both located to the west of the Magallanes-Austral Basin, while Pankhurst et al. (2000) proposed that volcanic rocks of the Tobifera Formation contributed Early to Late Jurassic zircons (201–145 Ma). The Southern Patagonian Batholith along the southwestern and western side of the basin experienced 3 plutonic episodes dating between 144 and 137 Ma, 136–127 Ma, and 126–75 Ma, providing zircons of these ages (Hervé et al., 2007).

Zircon populations in the Sierra Baguales can be broadly classified into 7 groups, namely I, between 3000 and 1000 Ma; IIe, between 700 and 250 Ma; IIw, between 700 and 200 Ma; IIIe, between 160 and 65 Ma; IIIw, between 155 and 75 Ma; IV, between 50 and 30 Ma; and V, between 25 and 15 Ma. The designations e (east) and w (west) indicate zircons of similar age ranges but different source areas as suggested by palaeocurrent directions. In the western source area groups, there are gaps between 1000–700 Ma, 200–155 Ma, 75–50 Ma, and 30–25 Ma, whereas the eastern provenance area groups show gaps between 250–160 Ma, and 65–50 Ma. In the southern part of the Magallanes-Austral Basin, the zircons dated by Sánchez et al. (2010) from the “Cabo Nariz Beds” range between 165 and 57 Ma, thus roughly coinciding with group IIIe zircons. Three zircon ages fall in group II and two in group I. In the Chorillo Chico Formation near Punta Arenas, which is chronostratigraphically equivalent to the “Cabo Nariz Beds”, we only found group IIIe zircons.

The Tres Pasos Formation hosts zircons belonging to groups I, IIe and IIIe, which according to palaeocurrent studies and lateral facies changes were derived from source areas to the north of the Magallanes-Austral Basin. Bernhardt (2011) also considered some input from the Andean Fold-and-Thrust Belt to the west. As far as group I zircons is concerned, outcrops of basement rocks with ages exceeding 1000 Ma are scarce in southern South America, currently only known to be present northeast

### Zr-LF-002

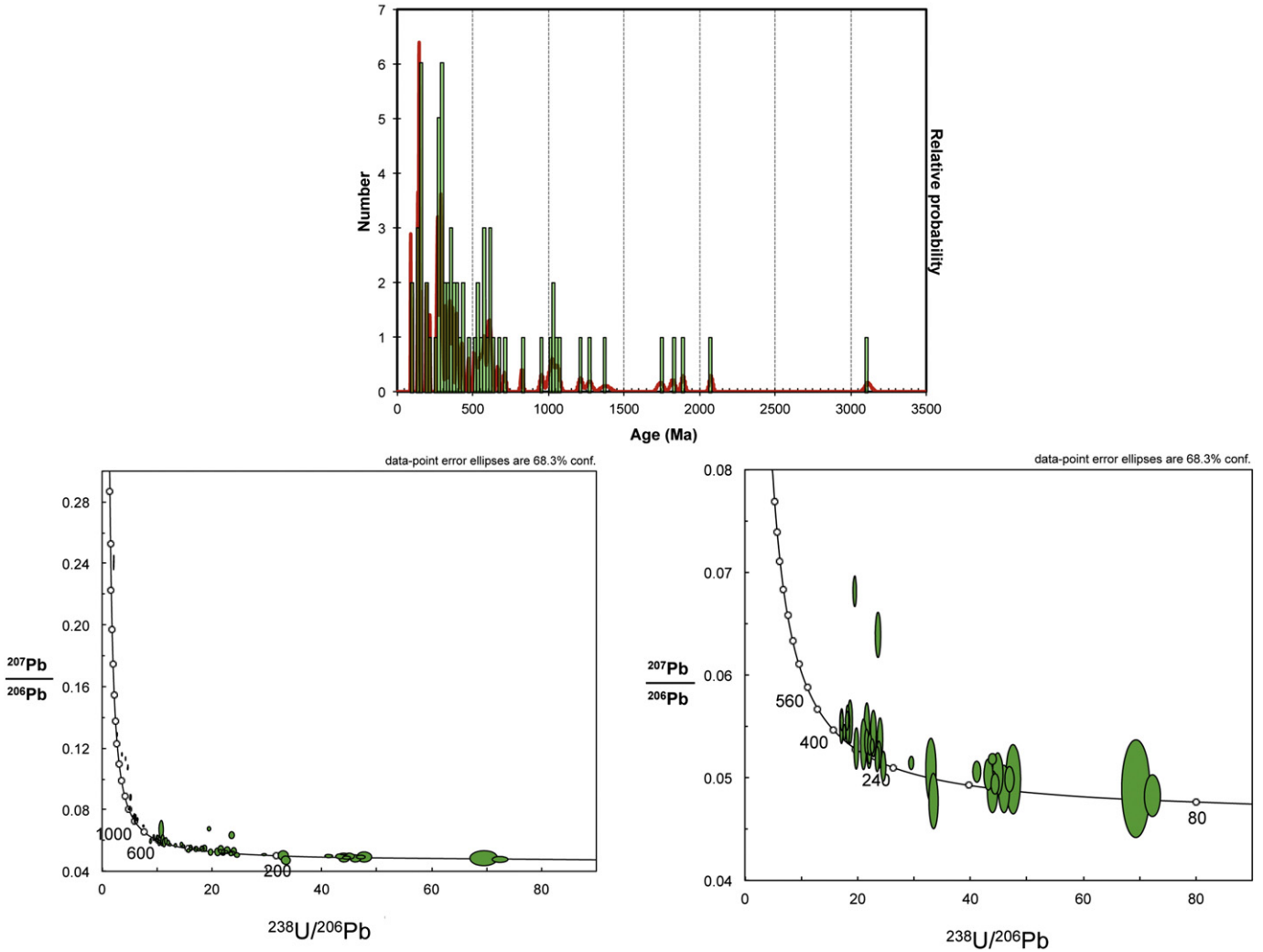


Fig. 14. U-Pb detrital zircon ages in sample ZR-LF-002 from the Santa Cruz Formation (after Bostelmann et al., 2013).

of the Magallanes-Austral Basin in the Río de la Plata Craton where ages between 2200 and 2000 Ma are recorded (Santos et al., 2003; Ramos et al., 2014a, 2014b), and in the North Patagonia Massif where relatively high-grade schists and gneisses with Rb-Sr ages of up to 1190 Ma (Linares et al., 1988) are intruded by Paleozoic granites (Pankhurst et al., 1998). The Kalahari Craton of southern Africa also has Mesoproterozoic rocks (1600–1000 Ma), whereas the Proto-Kalahari Craton dates back to the Archaean (Jacobs et al., 2008). The Magallanes-Austral Basin was at about the same distance from the Kalahari and Río de la Plata Cratons during the Jurassic, so that detritus derived from the northeast could have been diverted into its north-south trending axis.

Some of the group IIe zircons in the Tres Pasos Formation could have been sourced by the Deseado Massif (Fig. 1; 16), where small windows in the Jurassic sequence reveal micaceous and amphibolitic schists of very late Precambrian or Cambrian age, as well as Permo-Triassic plutonic rocks located to the north of the Magallanes-Austral Basin at 40°S (Pankhurst et al., 1998).

The Dorotea Formation, despite being the oldest unit for which zircon data are available in the Sierra Baguales, did not yield zircons representing group I, and obviously also lacks groups IV and V. However, 3 zircons belonging to group I were dated by us in samples from Cerro Castillo. This formation therefore contains groups I, IIe and IIIe. On the other hand, group I zircons do appear to be absent from the

Man Aike Formation, as we found only groups IIe, IIIe and IV in Sierra Baguales, whereas the time-equivalent Loreto Formation in the vicinity of Punta Arenas yielded only groups IIIe and IV. It therefore seems that the Dorotea Formation still received some detritus from the Río de la Plata Craton or time-equivalent rocks to the north-northeast, but that this source area became obsolete during deposition of the Man Aike Formation, in which groups IIe, IIIe, and IV are strongly represented.

Although group IIe zircon ages (636–268 Ma) partially overlap with the maximum recorded ages (451–267 Ma) in the Eastern Andes Metamorphic Complex, 62% of the published ages of metamorphic complexes west of the Magallanes-Austral Basin (Hervé et al., 2008; fig. 1) fall in the gap of 250–160 Ma between groups IIe and IIIe. Moreover, zircons between 636 and 451 Ma are represented neither in these metamorphic complexes nor in the Southern Patagonian Batholith. Although group IIIe (160–65 Ma) zircons could have been derived from the latter, where the oldest recorded intrusion age is 157 Ma (Hervé et al., 2007), a source located to the west would contradict the majority of measured palaeocurrent directions.

The region northeast and east of the Magallanes-Austral Basin has a magmatic and metamorphic belt with Paleozoic basement and sedimentary rocks as well as granitoid intrusions, which could have contributed some of the group IIe zircons to the Dorotea and Man Aike Formations (Fig. 16). This prominent geomorphological feature, the



## Zr-LF-001

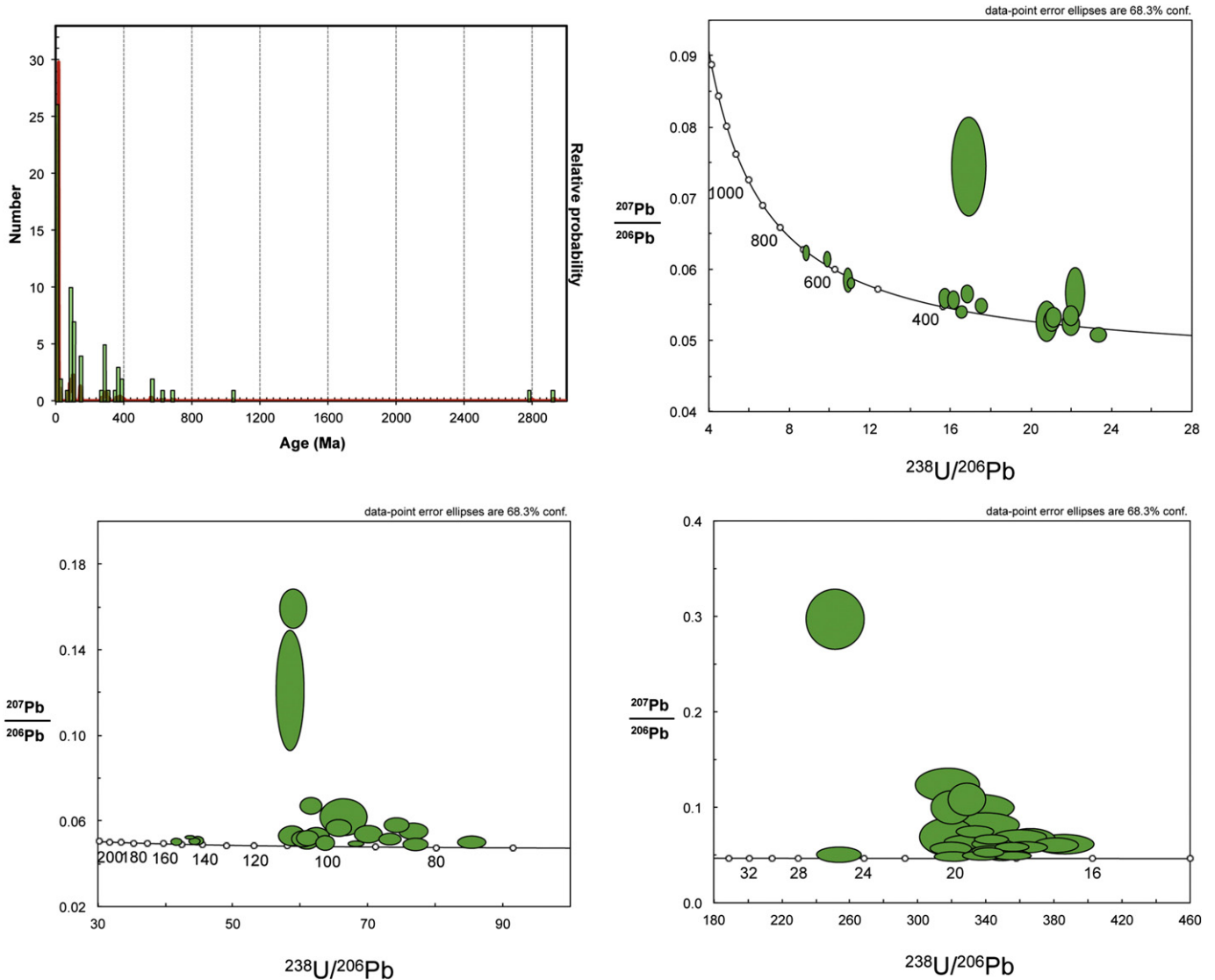


Fig. 15. U-Pb detrital zircon ages in sample ZR-LF-001 from the Santa Cruz Formation (after Bostelmann et al., 2013).

Western Magmatic Arc (e.g. Ramos, 2008), is known as the Río Chico-Punta Dúngenes Arc in its offshore, southeastern extension (Galeazzi, 1996; fig. 1; 16). The Western Magmatic Arc has plutonic and metamorphic rocks in which ages between 476 Ma and 344 Ma have been recorded (Ramos, 2008), and according to this author (Fig. 10) shed detritus westward into the Magallanes-Austral Basin. Another granite pluton in the Western Magmatic Arc with an age of 280 Ma (Ramos, 2008) could have contributed some of the younger zircons to group IIe. On the other hand, older zircons could have been derived from the Deseado Massif, which is situated between the Western Magmatic Arc and Magallanes-Austral Basin (Fig. 16) and where ages between 580 and 346 Ma have been recorded (Permuy Vidal et al., 2014). Basement rocks with ages between 536 and 527 Ma also occur to the southwest of Puerto Dúngenes (Fig. 16) (Hervé et al., 2008; Dickinson, 2009).

Alternatively, Jurassic and Cretaceous zircon populations identified in the Dorotea and Man Aike Formations could have been eroded from the rhyolitic Chon-Aike Province (Fig. 16), which overlaps with the Magallanes-Austral Basin and has plutons with the same ages (Gust et al., 1985; Pankhurst and Rapela, 1995). Some of the zircons in the Man Aike Formation could also have been reworked from the underlying Dorotea Formation, because it shows ample evidence of reworked fossils (e.g. shark

teeth) from the latter formation and their contact is a prominent erosional unconformity.

The origin of group IIIe zircons (160–65 Ma) in the Dorotea, Man Aike, and Chorillo Chico Formations is more problematic if sources southeast of the Magallanes-Austral Basin are to be considered because of the recorded palaeocurrent directions. The basin does extend south-eastward to the Magallanes-Fagnano Fault System in Fuegian Patagonia where it links up with the Falkland-Malvinas Basin, so that transport could easily have taken place along the basin axis (Fig. 16). However, this implies the existence of a hitherto unidentified point source in the vicinity of the present Cape Horn.

Finally, group IV zircons (50–30 Ma) in the Man Aike Formation were possibly eroded from intrusions of this age around the western exit of the Magellan Strait (Hervé et al., 2007), as some palaeocurrents suggest a possible source to the southwest (Fig. 10B).

In the Río Leona Formation both groups I and II zircons are absent, while groups IIIw and IV are well represented. Plutons with Jurassic-Cretaceous ages that could have provided group IIIw zircons (155–75 Ma) to the Río Leona Formation are common west of the Magallanes-Austral Basin (Fildani et al., 2003; Hervé et al., 2007). The majority are emplaced into the western flank of the Southern Patagonian

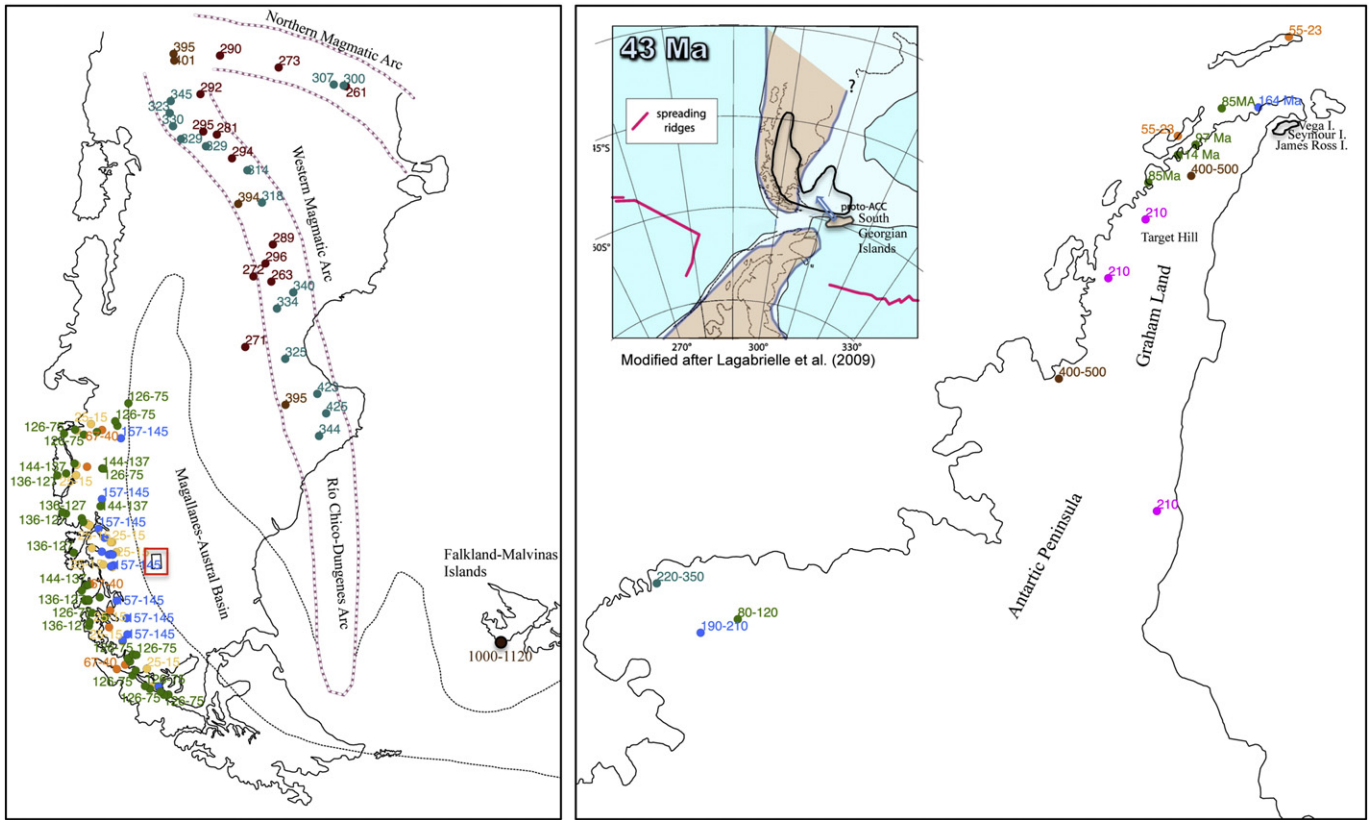


Fig. 16. Distribution of possible detrital zircon source rocks in southern South America and the Antarctic Peninsula. See text for references.

Andes where they form part of the Southern Patagonian Batholith, for example east of the Madre de Dios Archipelago and Duke de York Island around 50°–51°S, at the same latitude as the Sierra Baguales (Fig. 16). In this sector the vast majority of the plutons are of Jurassic to Cretaceous and Neogene age, with only one Paleogene date, which coincides with the zircon age gap between 67 and 49 Ma in the Río Leona Formation.

The absence of group IIe, having been replaced by group IIw in the Río Leona Formation, suggests that the source area had begun to shift by this time, but that group IV was still being contributed. The source of the latter was probably situated between the Pacific end of the Magallanes Strait and the Guadalupe Channel to the north, i.e. to the southwest of the Sierra Baguales (Fig. 16).

The Estancia 25 de Mayo Formation lacks groups I, IIw and IIIw, hosting only group IV, which reflects the dominance of the southwestern provenance that contributed to the Río Leona Formation.

The Santa Cruz Formation has zircons of group I, IIw, IIIw and V, being the only formation in the Sierra Baguales with group I zircons. In this case the Kalahari and Río de la Plata Cratons can be discarded as direct sources due to the recorded northwesterly palaeocurrent trend in the Santa Cruz Formation. However, the reworking of Jurassic and Cretaceous successions, such as the Tobífera, Zapata, Punta Barrosa and Cerro Toro Formations, which do have outcrops to the southwest and west of the Sierra Baguales, could have provided detrital zircons of Precambrian age, as such zircons are known to be present within these rocks. The erosion of these successions implies significant uplift and probably folding to the southwest and west of the Sierra Baguales, which would coincide with the observed change in palaeocurrent directions.

Finally, zircons of Neogene age ranging from 25 Ma to 15 Ma (group V) coincide with early to middle Miocene plutons dated by Hervé et al. (2007) in the Southern Patagonian Batholith between 50° and 51°S, directly to the west of the Sierra Baguales (Fig. 16).

### 8. Palaeobotany and palaeoclimate

A quantitative reconstruction of terrestrial paleoclimate can be made using fossil leaf morphology (e.g. Wolfe, 1995; Wilf, 1997; Mosbrugger and Utescher, 1997; Mosbrugger, 1999; Kowalski, 2002; Uhl et al., 2007). Estimations of the mean annual precipitation (MAP), mean annual temperature (MAT), and diversity according to the number of morphospecies, were based on 3746 fossil leaves collected at the localities of Barranca de las Hojas and Alto Río Bandurrias in the Río Leona Formation (Fig. 1). The fossil flora of this formation were compared to 4 fossil flora sites (Fig. 1) in Patagonia ranging in age from Paleocene to Eocene, which had been used previously to estimate the MAP and MAT as well as the diversity conditions (Wilf et al., 2005; Hinojosa et al., 2006; Iglesias et al., 2007). The Palacio de los Loros fossil flora of Paleocene age (61.7 Ma) represent a MAP of 166.3 cm, a MAT of 12.2 °C, and a diversity of 39 morphospecies (Hinojosa et al., 2006; Iglesias et al., 2007). The Early Eocene fossil flora of Ligorio Marquez (Hinojosa et al., 2016) indicate a MAP of 108–153 cm and a MAT between 17.2 °C and 20.9 °C, with a diversity of 55 morphospecies (Hinojosa et al., 2006, 2016). At Laguna el Hunco, the fossil floras are of early Eocene age (52 Ma), reflecting a MAP of 193.8 cm, a MAT between 14.8° and 17.7 °C, and a diversity of 122 morphospecies (Wilf et al., 2005; Hinojosa et al., 2011; Peppe et al., 2011; Quattrocchio et al., 2013). Finally, the fossil flora of Río Turbio, with a middle Eocene age (45 Ma) indicate a MAP of 152.5 cm, a MAT between 16.1 and 18 °C, and a diversity of 45 morphospecies (Hinojosa, 2005; Hinojosa et al., 2011; Peppe et al., 2011; Quattrocchio et al., 2013).

Our data indicate that the Río Leona Formation, with a Rupelian (early Oligocene) age, reflects a MAP of 55–74 cm based on multivariate analysis, and 92–96 cm according to the univariate method. As concerns the MAT, we estimate a range of 6.7 °C–7.7 °C according to the standard equations for Chile (MAT = 18.85 \* pE + 3.83) and South America (MAT = 26.03 \* pE + 1.31) (Hinojosa et al., 2011) and between 7.6

and 11 °C according to CLAMP (Climate Leaf Analysis Multivariate Program) (Wolfe, 1993, 1995; Kovach and Spicer, 1995; Wolfe and Spicer, 1999; Spicer, 2000; Spicer et al., 2004) including the CLAMP3bSA dataset (Hinojosa, 2005). Diversity in the Río Leona Formation includes a total of 24 dicotyledoneous morphospecies, in which the families *Nothofagaceae*, *Mirtaceae*, *Cunoniaceae*, *Sapindaceae*, *Gesneriaceae*, *Leguminosae*, *Monimiaceae*, *Grosulariaceae*, *Berberidaceae*, *Blechnaceae*, and *Podocarpaceae* stand out. These have a typical Mixed Flora phytogeographic character and indicate the oldest cold and dry forests in Patagonia.

The MAP, MAT and diversity conditions mentioned above illustrate the palaeoclimatic evolution and composition of forests in Patagonia, where Paleocene–Eocene, high-diversity forests flourishing under high precipitation and temperature conditions during the Eocene were replaced by low-diversity forests with low MAP and MAT conditions during the early Oligocene (Fig. 17).

The decrease in temperature recorded in the fossil flora of the Río Leona Formation between the Lutetian/Bartonian and early Oligocene coincides with the opening of the Drake Passage, which caused the first influx of Pacific sea-water into the Atlantic Ocean (Scher and Martin, 2006) and the development of the Antarctic Circumpolar Current (Barker, 2001). This event rang in the start of glaciation in Antarctica, as manifested in the global Oi-1 sea level fall (Zachos et al., 1996), an increase in deep-sea  $\delta^{18}\text{O}$ , and a decrease in atmospheric  $\text{CO}_2$  (Zachos et al., 2001; Beerling and Royer, 2011). This cooling period, referred to as the Bartonian–Rupelian Cooling by Le Roux (2012a, 2012b), was not only subcontinent-wide but global. Independent records of palynomorph species diversity in the Río Leona Formation (Barreda et al., 2009) also indicate a decrease in temperature, and a similar trend is observed during the Cenozoic at tropical latitudes (Jaramillo et al., 2006).

On the other hand, the precipitation registers a decrease from 150 to 200 cm during the Paleocene and Eocene to less than 80 cm (55–70 cm) during the Oligocene. This decrease in precipitation went hand-in-hand with a decrease in morphospecies diversity in Patagonia, passing from 39 to 131 in the Paleocene fossil flora of Palacio de los Loros and the Eocene fossil flora of Laguna el Hunco, to only 29 morphospecies in the palaeoflora of the Río Leona Formation. The decrease in precipitation and morphospecies diversity in the Sierra Baguales can be related to the rise of the Southern Patagonian Andes as an orographic barrier to the Westerly Winds and creating a rain shadow to the east thereof, which is consistent with the abrupt change in palaeocurrent directions and zircon source areas between the Priabonian and Rupelian (~34 Ma). Topographic forcing on climate only begins to take effect at around 1000 m (Browning, 1980), so that this amount of uplift would have represented a major pulse in the Andean tectonic cycle. Palaeocurrents from the southwest at this time also agree with the present strike and dip of the Sierra Baguales strata, which are mainly tilted towards the northeast. It can therefore be postulated that tectonic compression at this time was directed from the southwest. At Cabo Nariz in Bahía Inútil (Fig. 1), our measured mean strike of 292° is consistent with this trend.

## 9. Discussion and conclusions

The different lines of evidence presented above, including the recorded changes in depositional environments, palaeocurrent directions, zircon source areas, and palaeoclimate, all coincide in the following sequence of tectonic events:

During the Late Cretaceous the depositional environment changed from a continental slope system with turbidites in the Tres Pasos Formation to deltaic conditions in the overlying Dorotea Formation. This shallowing-upward succession suggests that tectonic uplift started during the late Campanian. Palaeocurrents were rather variable with a full range between northeast and southeast, but being mainly from the east. The most probable source consisted of the Western Magmatic

and Río Chico–Punta Dúngenes Arcs (as previously proposed by Ramos, 2008), as well as the rhyolitic Chon-Aike Province.

Tectonic uplift continued after deposition of the Dorotea Formation, causing a 30 m.y.–long period of erosion that lasted throughout the Paleocene and most of the Eocene (~70–40 Ma), ending with the deposition of the Man Aike Formation. The latter succession still received its detritus from the east and southeast, suggesting that the erosion was caused by tectonic uplift focused in this area. Although the eastern provenance can possibly still be attributed to the Río Chico–Punta Dúngenes Arc, the southeastern source needs another explanation. We propose that a local continental plate fragment was attached to the eastern end of Fuegian Patagonia and immediately to the south of the Falkland–Malvinas Plateau Basin. Our zircon data suggest that it may have formed part of the Antarctic Peninsula and/or its northeastern extension.

Zircon ages between 120 Ma and 80 Ma have been registered from the northern tip of the Antarctic Peninsula (Fig. 16) (Pankhurst, 1990). This area could also have contributed some group IIe zircons, as crystalline basement crops out at Target Hill and elsewhere in Graham Land (Fig. 16), where whole-rock ages of  $410 \pm 15$  and  $426 \pm 12$  Ma have been obtained (Milne and Millar, 1989).

The relative position of the Antarctic Peninsula with respect to southern South America during the Mesozoic and Cenozoic is still problematic (Miller, 2007), although many accept that it was located west of South America from the Middle to Late Jurassic (e.g., Grunow et al., 1987; Lawver and Scotese, 1987; Hanson and Wilson, 1991; Ghidella et al., 2002; Hervé and Fanning, 2003; Hervé et al., 2008; Breitsprecher and Thorkelson, 2009) and from there drifted southward along the South American Plate boundary. A problem with this interpretation is that Late Cretaceous and Cenozoic strike-slip faults in the Southern Patagonian Andes as well as on the eastern side of the Antarctic Peninsula are dominantly right-lateral (Storey and Nell, 1988; Diraison et al., 2000), which contradicts this notion. On the other hand, Seton et al. (2012; figs. 18–22) show the position of the Antarctic Peninsula as essentially unchanged to the south-southwest of Patagonia between 200 and 120 Ma, from where it drifted north and east, almost becoming a southward continuation of Fuegian Patagonia by 60 Ma. Diraison et al. (2000; fig. 3b and c) indicate this position to have been reached between 90 and 50 Ma, and that by the latter date, South Georgia was located along the northern boundary of the Scotia Plate. Several other authors have also indicated the position of the Antarctic Peninsula immediately to the south of Fuegian Patagonia during the Late Cretaceous (Barker and Lawver, 1988; Lagabrielle et al., 2009; Eagles, 2016a). It has also been suggested that the Antarctic Peninsula was a continuation of Fuegian Patagonia and Cordillera Darwin (Veevers et al., 1984; Pankhurst, 1990; Reguero et al., 2013) extending southeast of the Magallanes–Austral–Falkland–Malvinas Basin even during the Jurassic. However, Eagles (2016b) disputed the proximity of South Georgia to Tierra del Fuego during the Early Cretaceous.

An alternative northeastern extension of the Antarctic Peninsula is the small subsided banks of the Scotia Sea, including Terror Rise, Pirie Rise, and Bruce Bank, which Eagles and Jokat (2014) referred to as Omond Land. Given their present proximity to the Antarctic Peninsula and the South Orkney microcontinent, these could perhaps be more easily reconciled with the postulated southeastern source, which would have been removed by extension, rupture and subsidence during the Eocene.

If our proposal is correct that the northernmost tip of the Antarctic Peninsula and/or its northeastern extension was located immediately southeast of the Magallanes–Austral Basin during the Lutetian, this could have provided detritus to the Man Aike Formation along the northwest-trending basin axis. Uplift here could have been caused by the development of a transform fault with accompanying shoulder elevation, which can easily reach more than 1 km (Buck, 1986; Basile and Allemand, 2002). The most likely candidate here is the North Scotia Ridge, a left-lateral transform boundary forming the eastward extension

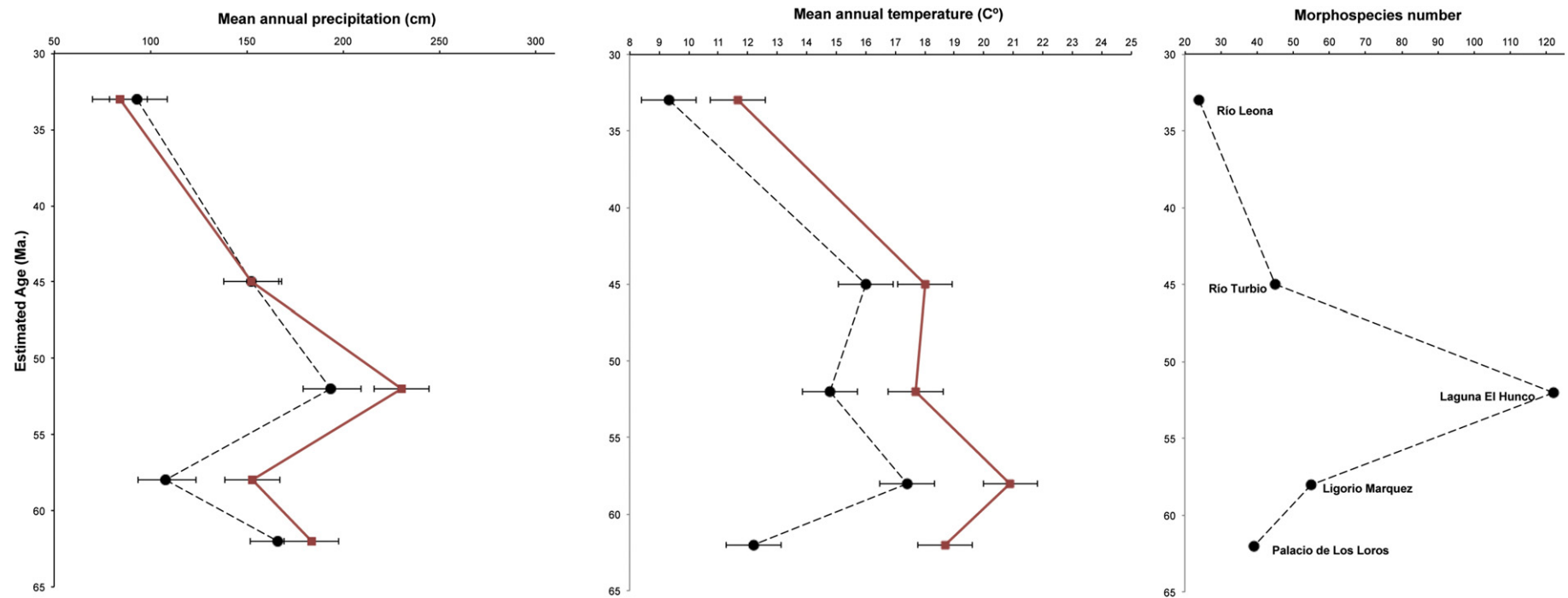


Fig. 17. Palaeoclimatic and palaeodiversity evolution in Patagonia as derived from fossil leaf morphology.

of the Magallanes–Fagnano Fault System in Fuegian Patagonia and stretching east to South Georgia, with a series of shallow banks in between (Eagles and Jokat, 2014). Geophysical surveys indicate that this ridge consists of mainly continental blocks, suggesting post-Cretaceous fragmentation of a formerly continuous continental area (Barker and Griffiths, 1972). It is still unclear whether the South Georgian Islands, presently located on the South American side of the plate boundary, are part of the Scotia Plate or have been recently accreted to the South American Plate (Thomas et al., 2003), but they could present vestiges of such an uplift shoulder. The original position of the South Georgia microcontinent was south of the Burdwood Bank and south of the Falkland–Malvinas Islands, from where it moved further east during the ongoing lengthening of the North Scotia Ridge (Dalziel et al., 2013). Considering the left-lateral movement along this ridge, this would imply that it was originally part of the Antarctic/Scotia Plate and could thus have formed, together with the submerged banks mentioned above, the northeastern extension of the Antarctic Peninsula. The Scotia Plate was formed mainly since a change in relative motion between the South American and Antarctic Plates during the Ypresian (~50 Ma) according to Pelayo and Wiens (1989). Marine geophysical data indicate that motion between the South American and Antarctic Plates at that time shifted from N–S to WNW–ESE, which was accompanied by an eightfold increase in the separation rate (Livermore et al., 2005).

There are many palaeontological similarities between the Antarctic Peninsula and the Magallanes–Austral Basin. For example, Aristonectinae (Plesiosauroidea) found in the Sierra Baguales are also found on Seymour Island (Gasparini et al., 1984; Chatterjee and Small, 1989; Fostowicz-Frelik and Gaździcki, 2001), James Ross Island (Otero et al., 2014) and Vega Island (O’Gorman et al., 2010) of the Antarctic Peninsula. South Pacific records are so far restricted to the Quiriquina Basin of central Chile, which according to Cecioni (1970) and Le Roux (2012a) was connected to the Magallanes–Austral Basin during the Late Cretaceous. However, plesiomorphic elasmosaurids were present in both the latter basin and the Antarctic Peninsula during the early Campanian, but only appeared in the Quiriquina Basin during the early Maastrichtian (Otero et al., 2015). Furthermore, palaeoichthyofauna of North Atlantic affinity present in both the Magallanes–Austral Basin and on Seymour Island include the chondrichthyan genera *Squatina*, *Pristiophorus*, and *Carcharocles* (Otero et al., 2013; Kriwet et al., 2016). Chondrichthyans were dominant elements in the Antarctic fish fauna during the Paleogene, but decreased in abundance from the middle to late Eocene, during which time bony fishes increased. This decline of chondrichthyans as registered in the Eocene La Meseta Formation on Seymour Island was related to the sudden cooling of seawater, reduction in shelf area, and increasing shelf depth according to Kriwet et al. (2016). Although these authors attributed their disappearance during the late Eocene to climatic conditions rather than plate tectonics, it could also be due to the development of a transform fault and ridge between southernmost South America and the northern tip of the Antarctic Peninsula. Lagabrielle et al. (2009) in fact show the latter immediately to the south of Patagonia at 43 Ma, from where it drifted to the east until 32 Ma, accompanied by strengthening of the Antarctic Circumpolar Current. Up to 25 Ma it was still drifting eastward along the Magallanes–Fagnano Transform Fault–Northern Scotia Ridge stretching from Fuegian Patagonia to the southern border of the Falkland–Malvinas Plateau, from where it began to move south with the development of an ocean ridge in the Drake Passage.

Palaeomagnetic studies indicate that the Antarctic Peninsula-block was located at or near its present-day position with respect to East Antarctica by ~130 Ma, while Antarctic Peninsula-block ~110 and ~85 Ma poles are similar to equivalent age poles from the East Antarctica-block, indicating that little or no relative motion between these two blocks occurred (Grunow, 1993). Poblete et al. (2011) also concluded from their palaeomagnetic studies in the Antarctic Peninsula that the small displacement between the latter and the East Antarctica-block during the Tertiary is probably not discernible by palaeomagnetism.

Furthermore, Mid-Cretaceous poles in the northern and southern parts of the Antarctic Peninsula are alike, suggesting that the “S” shape of the peninsula was not due to oroclinal bending since 110 Ma (Grunow, 1993). Fitting the Antarctic Peninsula along the western border of the South American Plate during the Late Cretaceous would therefore require considerable counterclockwise rotation of both the former and East Antarctica to bring them into their present position and orientation. This should also be manifested in left-lateral instead of the observed right-lateral strike-slip faulting along the western side of South America and the eastern side of the Antarctic Peninsula. However, if the Antarctic Peninsula was initially located south-southwest of South America and then drifted north-northeast to become attached to the southeastern tip of Patagonia, it would explain the left-lateral strike-slip direction along the Magallanes–Fagnano Fault System and North Scotia Ridge. The right-lateral strike-slip faulting observed at the eastern side of the Antarctic Peninsula could be due to its southwestward drift along the South Scotia Ridge after separation from the South Georgian–Falkland–Malvinas continental fragment. This whole process would require very little rotation to bring it into its present orientation, which would agree with the 10° postulated by Poblete et al. (2011). The Man Aike Formation was deposited in a coastal (estuarine) environment, which indicates that uplift of the postulated ridge shoulder between the Scotia and South American Plates had come to an end by 40 Ma and that denudation or minor subsidence brought the region closer to base level.

Renewed uplift followed during deposition of the Río Leona Formation, maintaining a continental environment close to base level until the Rupelian (early Oligocene). The source areas by now had shifted to the southwest, reflecting the initial uplift of the Southern Patagonian Andes at around 34 Ma. This uplift led to the development of a rain shadow to the east of the latter, causing a marked decrease in precipitation. It was accompanied by a drop in temperature and a decrease in morphospecies diversity, which was also reflected globally at the time. This can be attributed to the complete separation of the Antarctic Peninsula from South America, with the final opening of the Drake Passage that allowed the generation of the Antarctic Circumpolar Current and the Bartonian–Rupelian Cooling period leading to the glaciation of Antarctica (Le Roux, 2012a).

A period of crustal subsidence occurred at around 19 Ma that caused the Patagonian Transgression, as reflected in the marine Estancia 25 de Mayo Formation. This was followed by a period of accelerated plate convergence together with slab detachment at around 17 Ma, causing another period of rapid uplift in the Southern Patagonian Andes. Apatite fission track ages from the western flank of the Andean segment suggest that 3–4 km of denudation occurred in this region since 17 Ma (Blisniuk et al., 2006). This uplift bought the Sierra Baguales area above base-level and led to the establishment of the continental depositional environment of the Santa Cruz Formation. Zircons probably derived from older, underlying formations were now being exposed to the west, suggesting that folding accompanied this uplift.

## Acknowledgements

This research was financially supported by Project ANILLOS ATC-105 and Projects FONDECYT 1130006 and 1150690, being carried out under the auspices of Project CONICYT/FONDAP 15090013. N.M.G. is grateful for the grant “Beca CONICYT de Estudios de Doctorado para Extranjeros en Chile”. Detrital zircon dating was carried out by Mathieu Leisen in the Mass Spectrometry Laboratory of the Andean Geothermal Centre of Excellence. Victor Ramos and an anonymous reviewer provided much-appreciated comments which helped to improve this manuscript considerably.

## References

- Barbeau Jr., D.L., Olivero, E.B., Swanson-Hysell, N.L., Zahid, K.M., Murray, K.E., Gehrels, G.E., 2009. Detrital-zircon geochronology of the eastern Magallanes foreland basin:

- implications for Eocene kinematics of the northern Scotia Arc and Drake Passage. *Earth Planet. Sci. Lett.* 284, 489–503.
- Barker, P.F., 2001. Scotia regional tectonic evolution: implication for the mantle flow and paleocirculation. *Earth-Sci. Technol. Eng.* 55, 1–39.
- Barker, P.F., Griffiths, D.H., 1972. The evolution of the Scotia Ridge and Scotia Sea. *Philos. Trans. R. Soc. A Math. Phys. Eng. Sci.* 271, 1213.
- Barker, P.F., Lawver, L.A., 1988. South American–Antarctic plate motion over the past 50 Myr, and the evolution of the South American–Antarctic ridge. *Geophys. J. Int.* 94, 377–386.
- Barreda, V., Palazzesi, L., Marensi, S., 2009. Palynological record of the Paleogene Río Leona Formation (southernmost South America): stratigraphical and paleoenvironmental implications. *Rev. Palaeobot. Palynol.* 154, 22–33.
- Basile, C., Allemand, P., 2002. Erosion and flexural uplift along transform faults. *Geophys. J. Int.* 151, 646–653.
- Beerling, D.J., Royer, D.L., 2011. Convergent Cenozoic CO<sub>2</sub> history. *Nat. Geosci.* 4, 418–420.
- Bernhardt, A., 2011. Paleogeography and Sedimentary Development of Two Deep-marine Foreland Basins: The Cretaceous Magallanes Basin, Southern Chile, and the Tertiary Molasse Basin, Austria. Unpubl. Ph.D. thesis, Stanford University (218 pp.).
- Bernhardt, A., Jobe, Z.A., Lowe, D.R., 2008. The evolution of an elongate foreland basin: the deep to shallow-marine filling of the Cretaceous Magallanes Basin, Chile. 28th Annual GCSSEPM Foundation, Bob F. Perkins Research Conference, pp. 268–310.
- Bernhardt, A., Jobe, Z.A., Lowe, D.R., 2011. Stratigraphic evolution of a submarine channel-lobe complex system in a narrow fairway within the Magallanes foreland basin, Cerro Toro Formation, southern Chile. *Mar. Pet. Geol.* 28, 785–806.
- Biddle, K.T., Uliana, M.A., Mitchum Jr., R.M., Fitzgerald, M.G., Wright, R.C., 1986. The stratigraphic and structural evolution of the central and eastern Magallanes Basin, southern South America. In: Allen, P.A., Homewood, P. (Eds.), *Foreland Basins*. International Association of Sedimentologists, Special Publication 8, pp. 41–63.
- Błisniuk, P.M., Stern, L.A., Chamberlain, C.P., Zeitler, P.K., Ramos, V.A., Sobel, E.R., Haschke, M., Strecker, M.R., Warkus, F., 2006. Links between mountain uplift, climate, and surface processes in the southern Patagonian Andes. *The Andes, Active Subduction Orogeny*. Ch. 20, *Frontiers in Earth Sciences*. Springer Verlag, Berlin, pp. 429–440.
- Bossi, G.E., Vides, M.E., Ahumada, A.L., Georgieff, S.M., Muruaga, C.M., Ibañez, L.M., 2000. Análisis de las paleocorrientes y de la varianza de los componentes a tres niveles, Neógeno del valle del Cajón, Catamarca, Argentina. *Rev. Asoc. Argent. Sedimentol.* 7, 23–47.
- Bostelmann, E., Le Roux, J.P., Oyarzún, J.L., Gutiérrez, N., Vasquez, A., Carreño, C., 2012. A new continental Late-Early Miocene (Burdigalian) fossil fauna from the Sierra Baguales, Magallanes, Chile. III Simposio – Paleontología en Chile, Punta Arenas, Chile.
- Bostelmann, J.E., Le Roux, J.P., Vasquez, A., Gutiérrez, N.M., Oyarzún, J.-L., Carreño, C., Torres, T., Otero, R., Llanos, A., Fanning, C.M., Hervé, F., 2013. Burdigalian deposits of the Santa Cruz Formation in the Sierra Baguales, Austral (Magallanes) Basin: age, depositional environment and vertebrate fossils. *Andean Geol.* 40, 458–489.
- Breitsprecher, K., Thorkelson, D.J., 2009. Neogene kinematic history of Nazca–Antarctic–Phoenix slab windows beneath Patagonia and the Antarctic Peninsula. *Tectonophysics* 464, 10–20.
- Browning, K.A., 1980. Structure, mechanism and prediction of orographically enhanced rain in Britain. In: Hide, R., White, P.W. (Eds.), *Orographic Effects in Planetary Focus*. Global Atmospheric Research Programme Series 23, pp. 85–114.
- Buck, W.R., 1986. Small-scale convection induced by passive rifting: the cause for uplift of rift shoulders. *Earth Planet. Sci. Lett.* 77, 362–372.
- Calderón, M., Fildani, A., Herve, F., Fanning, C.M., Weislogel, A., Cordani, U., 2007. Late Jurassic bimodal magmatism in the northern sea-floor remnant of the Rocas Verdes basin, southern Patagonian Andes. *J. Geol. Soc. Lond.* 162, 1011e1022.
- Cecioni, G., 1957. Età della flora del Cerro Guido e stratigrafia del Departamento Última Esperanza. *Boll. Soc. Geol. Ital.* 76, 3–16.
- Cecioni, G., 1970. Esquema de Paleogeografía Chilena. Editorial Universitaria, Santiago (144 pp.).
- Chatterjee, S., Small, B.J., 1989. New plesiosaurs from the Upper Cretaceous of Antarctica. In: Crame, J. (Ed.), *Origins and Evolution of the Antarctic Biota*. Geological Society, London Special Publication 47, pp. 197–215.
- Crane, W.H., Lowe, D.R., 2008. Architecture and evolution of the Paine channel complex, Cerro Toro Formation (Upper Cretaceous), Silla Syncline, Magallanes basin, Chile. *Sedimentology* 55, 979–1009.
- Cuitiño, J.J., 2011. Registro sedimentológico e isotópico de paleoambientes marinos y transicionales en el patagoniano (Mioceno) del Lago Argentino. Unpubl. Ph.D. thesis. Facultad de Ciencias Exactas y Naturales, Universidad de Buenos Aires.
- Cuitiño, J.J., Pimentel, M.M., Ventura Santos, R., Scasso, R.A., 2012. High resolution isotopic ages for the early Miocene “Patagoniense” transgression in Southwest Patagonia: stratigraphic implications. *J. South Am. Earth Sci.* 38, 110–122.
- Cuitiño, J.J., Ventura Santos, R., Muruaga, P.J.A., Scasso, R.A., 2015. Sr-stratigraphy and sedimentary evolution of early Miocene marine foreland deposits in the northern Austral (Magallanes) Basin, Argentina. *Andean Geol.* 42, 364–385.
- Cuitiño, J.J., Ventura Santos, R., Scasso, R.A., 2013. Insights into the distribution of shallow marine/estuarine early Miocene oysters from southwestern Patagonia: Sedimentologic and stable isotope constraints. *PALAIOS* 28, 583–598.
- Dalziel, I.W.D., 1986. Collision and cordilleran orogenesis: An Andean perspective. In: Coward, M.P., Ries, A.C. (Eds.), *Collision Tectonics*. Geological Society, London Special Publication 19, pp. 389–404.
- Dalziel, I.W.D., De Wit, M.J., Palmer, K.F., 1974. Fossil marginal basin in the southern Andes. *Nature* 250, 291–294.
- Dalziel, I.W.D., Lawver, L.A., Norton, I.O., Gahagan, L.M., 2013. The Scotia Arc: genesis, evolution, global significance. *Annu. Rev. Earth Planet. Sci.* 41, 767–793.
- Dickinson, W.R., 2009. Anatomy and global context of North American Cordillera. In: Kay, S.M. (Ed.), *Backbone of the Americas: Shallow Subduction, Plateau Uplift, and Ridge and Terrane Collision*. Geological Society of America, Memoir 204, pp. 1–60.
- Diraison, M., Cobbold, P.R., Gapais, D., Rossello, E.A., Le Corre, C., 2000. Cenozoic crustal thickening, wrenching and rifting in the foothills of the southernmost Andes. *Tectonophysics* 316, 91–119.
- Eagles, G., 2016a. Plate kinematics of the Rocas Verdes Basin and Patagonian orocline. *Gondwana Res.* 37, 98–109.
- Eagles, G., 2016b. Tectonic reconstructions of the southernmost Andes and the Scotia Sea during the opening of the Drake Passage. In: Ghiglione, M.C. (Ed.), *Geodynamic Evolution of the Southernmost Andes*. Springer Int. Publ. AG, Switzerland, pp. 75–108.
- Eagles, G., Jokat, W., 2014. Tectonic reconstructions for paleobathymetry in Drake Passage. *Tectonophysics* 611, 28–50.
- Feruglio, E., 1938. El Cretácico superior del lago San Martín (Patagonia) y de las regiones adyacentes. *Physis* 12, 293–342.
- Feruglio, E., 1949. Descripción Geológica de la Patagonia. Ministerio de Industria y Comercio de la Nación. Dirección General de Yacimientos Petrolíferos Fiscales 2, pp. 1–349.
- Fildani, A., Hessler, A.M., 2005. Stratigraphic record across a retroarc basin inversion: Rocas Verdes–Magallanes Basin, Patagonian Andes, Chile. *Geol. Soc. Am. Bull.* 117, 1596–1614.
- Fildani, A., Cope, T., Graham, S.A., Wooden, J., 2003. Initiation of the Magallanes foreland basin: timing of the southernmost Patagonian Andes orogeny revised by detrital zircon provenance analysis. *Geology* 31, 1081–1084.
- Fosdick, J.C., Bostelmann, J.E., Leonard, J., Ugalde, R., Oyarzún, J.L., Griffin, M., 2015a. Timing and rates of foreland sedimentation: new detrital zircon U/Pb geochronology of the Cerro Dorotea, Río Turbio, and Río Guillermo formations, Magallanes Basin. XIV Congreso Geológico Chileno, La Serena, Chile.
- Fosdick, J.C., Grove, M., Graham, S.A., Hourigan, J.K., Lovera, O., Romans, B.W., 2015b. Detrital thermochronologic record of burial heating and sediment recycling in the Magallanes foreland basin, Patagonian Andes. *Basin Res.* 27, 546–572.
- Fosdick, J.C., Romans, B.W., Fildani, A., Calderón, M.N., Bernhardt, A., Graham, S.A., 2011. Kinematic history of the Cretaceous–Neogene Patagonia fold-thrust belt and Magallanes foreland basin, Chile and Argentina (51°30’S). *Geol. Soc. Am. Bull.* 123, 1679–1698.
- Fostowicz-Frelik, Ł., Gaździcki, A., 2001. Anatomy and histology of plesiosaur bones from the Upper Cretaceous of Seymour Island, Antarctic Peninsula. In: Gaździcki, A. (Ed.), *Palaeontological Results of the Polish Antarctic Expeditions. Part III*. *Palaeontologia Polonica* 60, pp. 7–32.
- Furque, G., 1973. Descripción geológica de la Hoja 58b Lago Argentino. Boletín del Servicio Nacional Minero y Geológico 140. Servicio Nacional Minero y Geológico, Buenos Aires, pp. 1–49.
- Galeazzi, J.S., 1996. Cuenca de Malvinas. In: Ramos, V.A., Turic, M.A. (Eds.), *Geología y Recursos Naturales de la Plataforma Continental Argentina*. 13° Congreso Geológico Argentino y 3° Congreso de Exploración de Hidrocarburos, Buenos Aires, Relatorio 15, pp. 273–309.
- Gasparini, Z., Del Valle, R., Goñi, R., 1984. An *Elasmosaurus* (Reptilia, Plesiosauria) of the Upper Cretaceous in the Antarctic. *Boletín Del Instituto Antártico Argentino* 305, pp. 1–24.
- Ghidella, M.E., Yañez, G., LaBrecque, J.L., 2002. Revised tectonic implications for the magnetic anomalies of the Western Wedell Sea. *Tectonophysics* 347, 65–86.
- González, E., 2015. Estratigrafía secuencial y sedimentología de la Formación Dorotea (Maastrichtiano), sector Río de las Chinas, región de Magallanes y Antártica Chilena, Chile (50°S). Memoria, Departamento de Geología, Universidad de Chile.
- Grunow, A.M., 1993. New paleomagnetic data from the Antarctic Peninsula and their tectonic implications. *J. Geophys. Res.* 98 (13815–13813).
- Grunow, A.M., Kent, D.W., Dalziel, I.W.D., 1987. Mesozoic evolution of West Antarctica and the Weddell Sea Basin: new paleomagnetic constraints. *Earth Planet. Sci. Lett.* 86, 16–26.
- Gust, D.A., Biddle, K.T., Phelps, D.W., Uliana, M.A., 1985. Associated Middle to Late Jurassic volcanism and extension in southern South America. *Tectonophysics* 116, 223–253.
- Gutiérrez, N.M., Le Roux, J.P., Bostelmann, J.E., Oyarzún, J.L., Vásquez, A., Araos, J., Carreño, C., Ugalde, R., Otero, R., Fanning, C.M., Hervé, F., 2013. Geology and stratigraphy of Sierra Baguales, Última Esperanza Province, Magallanes, Chile. *Geosur 2013*, Viña del Mar, Chile.
- Hanson, R.E., Wilson, T.J., 1991. Submarine rhyolitic volcanism in a Jurassic proto-marginal basin; southern Andes, Chile and Argentina. *Geol. Soc. Am. Spec. Pap.* 265, 13–28.
- Hervé, F., Fanning, C.M., 2003. Early Cretaceous subduction of continental crust at the Diego de Almagro Archipelago, southern Chile. *Episodes* 26, 285–289.
- Hervé, F., Calderón, M., Faúndez, V., 2008. The metamorphic complexes of the Patagonian and Fuegian Andes. *Geol. Acta* 6, 43–53.
- Hervé, F., Massonne, H.-J., Calderón, M., Theye, T., 2004. Metamorphic P–T conditions of rhyolites in the Magallanes fold and thrust belt, Patagonian Andes. *Bollettino di Geofisica teórica ed applicata, Extended Abstracts, International Symposium on the Geology and Geophysics of the Southernmost Andes, the Scotia Arc and the Antarctic Peninsula, Trieste*, pp. 15–18.
- Hervé, F., Panthurst, R.J., Fanning, C.M., Calderón, M., Yaxley, G.M., 2007. The South Patagonian batholith: 150 my of granite magmatism on a static plate margin. *Lithos* 97, 373–394.
- Hinojosa, L.F., 2005. Cambios climáticos y vegetacionales inferidos a partir de Paleofloras Cenozoicas del sur de Sudamérica. *Rev. Geol. Chile* 32, 95–115.
- Hinojosa, L.F., Gaxiola, A., Perez, M.F., Carvajal, F., Campano, M.F., Quattrocchio, M., Nishida, H., Uemura, K., Yabe, A., Bustamante, R., Kalim, M.T., 2016. Non-congruent fossil and phylogenetic evidence on the evolution of climatic niche in the Gondwana genus *Nothofagus*. *J. Biogeogr.* 43, 555–567.
- Hinojosa, L.F., Pérez, F., Gaxiola, A., Sandoval, I., 2011. Historical and phylogenetic constraints on the incidence of entire leaf margins: insights from a new South American model. *Glob. Ecol. Biogeogr.* 20, 380–390.
- Hinojosa, L.F., Pesce, O., Yabe, A., Uemura, K., Nishida, H., 2006. Physiognomical analysis and paleoclimate of the Ligorio Márquez fossil flora, Ligorio Márquez Formation,

- 46°45'S, Chile. In: Nishida, H. (Ed.), Post Cretaceous Floristic Changes in Southern Patagonia, Chile. Chuo University, Tokyo, pp. 45–55.
- Hoffstetter, R., Fuenzalida, H., Cecioni, G., 1957. Lexique Stratigraphique International, Amérique Latine. Fascicule 7, Chili. Centre National de la Recherche Scientifique, Paris (444 pp.).
- Hubbard, S.M., Fildani, A., Romans, B.W., Covault, J.A., McHargue, T.R., 2010. High-relief slope clinoform development: insights from outcrop, Magallanes Basin, Chile. *J. Sediment. Res.* 80, 357–375.
- Hubbard, S.M., Romans, B.W., Graham, S.A., 2008. Deep-water foreland basin deposits of the Cerro Toro Formation, Magallanes Basin, Chile: architectural elements of a sinusoidal basin axial channel belt. *Sedimentology* 55, 1333–1359.
- Iglesias, A., Wilf, P., Johnson, K.R., Zamuner, A.B., Cúneo, N.R., Matheos, S.D., Singer, B.S., 2007. A Paleocene lowland macroflora from Patagonia reveals significantly greater richness than North American analogs. *Geology* 35, 947–950.
- Jacobs, J., Pisarevsky, S., Thomas, R.J., Becker, T., 2008. The Kalahari Craton during the assembly and dispersal of Rodinia. *Precambrian Res.* 160, 142–158.
- Jaramillo, C., Rueda, M., Mora, G., 2006. Cenozoic plant diversity in the Neotropics. *Science* 311, 1893–1896.
- Jobe, Z.R., Bernhardt, A., Lowe, D.R., 2010. Facies and architectural asymmetry in a conglomerate-rich submarine channel fill, Cerro Toro Formation, Sierra del Toro, Magallanes Basin. *J. Sediment. Res.* 80, 1085–1108.
- Katz, H.R., 1963. Revision of Cretaceous stratigraphy in Patagonian Cordillera de Última Esperanza, Magallanes Province, Chile. *Am. Assoc. Pet. Geol. Bull.* 47, 506–524.
- Kovach, W.L., Spicer, R.A., 1995. Canonical correspondence analysis of leaf physiognomy: a contribution to the development of a new palaeoclimatological tool. *Palaeoclimates* 1, 125–138.
- Kowalski, E.A., 2002. Mean annual temperature estimation based on leaf morphology: a test from tropical South America. *Palaeogeogr. Palaeoclimatol. Palaeoecol.* 188, 141–165.
- Kriwet, J., Engelbrecht, A., Mörs, T., Reguero, M., Pfaff, C., 2016. Ultimate Eocene (Priabonian) chondrichthyans (Holocephal, Elasmobranchii) of Antarctica. *J. Vertebr. Paleontol.* <http://dx.doi.org/10.1080/02724634.2016.1160911>.
- Lagabrielle, Y., Goddérís, Y., Donnadieu, Y., Malavieille, J., Suarez, M., 2009. The tectonic history of Drake Passage and its possible impacts on global climate. *Earth Planet. Sci. Lett.* 279, 197–211.
- Lawver, L.A., Scotese, C.R., 1987. A revised reconstruction of Gondwanaland. *Gondwana Six: Structure, Tectonics, and Geophysics. Geophysical Monograph Series 40. American Geophysical Union*, pp. 17–23.
- Le Roux, J.P., 1991. Paleocurrent analysis using Lotus 1–2–3. *Comput. Geosci.* 17, 1465–1468.
- Le Roux, J.P., 1992. Determining the sinuosity of ancient fluvial systems from paleocurrent data. *J. Sediment. Petrol.* 62, 283–291.
- Le Roux, J.P., 1994. The angular deviation in circular statistics as applied to the calculation of channel sinuosities. *J. Sediment. Res.* A64, 86–87.
- Le Roux, J.P., 2012a. A review of Tertiary climate changes in southern South America and the Antarctic Peninsula. Part 1: oceanic conditions. *Sediment. Geol.* 247–248.
- Le Roux, J.P., 2012b. A review of Tertiary climate changes in southern South America and the Antarctic Peninsula. Part 2: continental conditions. *Sediment. Geol.* 247–248, 21–38.
- Le Roux, J.P., Puratich, J., Mourgues, A., Oyarzún, J.L., Otero, R.A., Torres, T., Hervé, F., 2010. Estuary deposits in the Río Baguales Formation (Chattian-Aquitanean), Magallanes Province, Chile. *Andean Geol.* 37, 329–344.
- Linares, E., Cagoni, M.C., Do Campo, M., Ostera, H.A., 1988. Geochronology of metamorphic and eruptive rocks of southeastern Neuquén and northern Río Negro Provinces, Argentine Republic. *J. S. Am. Earth Sci.* 1, 53–61.
- Livermore, R., Nankivell, A., Eagles, G., Morris, P., 2005. Paleogene opening of Drake passage. *Earth Planet. Sci. Lett.* 236, 459–470.
- Macauley, R.V., Hubbard, S.M., 2013. Slope channel sedimentary processes and stratigraphic stacking, Cretaceous Tres Pasos Formation slope system, Chilean Patagonia. *Mar. Pet. Geol.* 41, 146–162.
- Macellari, C.E., Barrio, C.A., Manassero, M.J., 1989. Upper Cretaceous to Paleocene depositional sequences and sandstone petrography of southwestern Patagonia (Argentina and Chile). *J. S. Am. Earth Sci.* 2, 223–239.
- Malumián, N., 1990. Foraminíferos de la Formación Man Aike (Eoceno, Sureste Lago Cardiel), Provincia de Santa Cruz, Argentina. *Rev. Asoc. Geol. Argent.* 45, 365–385.
- Malumián, N., 1999. La sedimentación en la Patagonia Extraandina. In: Caminos, R. (Ed.)—Instituto de Geología y Recursos Minerales, Geología Argentina, Anales Vol. 29, pp. 557–578.
- Malumián, N., Nañez, C., 2011. The Late Cretaceous–Cenozoic transgressions in Patagonia and the Fuegian Andes: Foraminifera, paleoecology and paleogeography. *Biol. J. Linn. Soc.* 103, 269–288.
- Marensi, S.A., Casadio, S., Santillana, S.N., 2002. La Formación Man Aike al sur de El Calafate (Provincia de Santa Cruz) y su relación con la discordancia del Eoceno medio en la cuenca Austral. *Rev. Asoc. Geol. Argent.* 57, 341–344.
- Marensi, S.A., Limarino, C.O., Tripaldi, A., Net, L.I., 2005. Fluvial systems variations in the Río Leona Formation: tectonic and eustatic controls on the Oligocene evolution of the Austral (Magallanes) Basin, southernmost Argentina. *J. S. Am. Earth Sci.* 19, 359–372.
- Marensi, S.A., Santillana, S.N., Net, L.I., Rinaldi, C.A., 2000. Facies conglomeráticas basales para la Formación Río Leona al sur del lago Argentino, Provincia de Santa Cruz, Argentina. Resúmenes, II Congreso Latinoamericano de Sedimentología y VIII Reunión Argentina de Sedimentología. *Mar del Plata*, pp. 109–110.
- Martínez-Pardo, R., 1965. *Bolivinoidea draco dorreeni* FINLAY from the Magellan Basin, Chile. *Micropaleontology* 11, 360–364.
- Miller, H., 2007. History of views on the relative positions of Antarctica and South America: a 100-year tango between Patagonia and the Antarctic Peninsula. In: Cooper, A.K., Raymond, C.R. (Eds.), *Antarctica: A Keystone in a Changing World* – Online Proceedings of the 10th ISAES, USGS Open-File Report 2007–1047, Short Research Paper 041, p. 4.
- Milne, A.J., Millar, I.L., 1989. The significance of mid-Palaeozoic basement in Graham Land, Antarctic Peninsula. *J. Geol. Soc. Lond.* 146, 207–210.
- Mosbrugger, V., 1999. The nearest living relative method. In: Jones, T.P., Rowe, N.P. (Eds.), *Fossil Plants and Spores: Modern Techniques*. Geological Society, London, pp. 261–265.
- Mosbrugger, V., Utescher, T., 1997. The coexistence approach—a method for quantitative reconstructions of Tertiary terrestrial palaeoclimate data using plant fossils. *Palaeogeogr. Palaeoclimatol. Palaeoecol.* 134, 61–86.
- Muñoz, J., 1981. Geología y petrología de las rocas ígneas e inclusiones ultramáficas del sector SW de Meseta Las Vizcachas, Última Esperanza, Magallanes, XII Región, Chile. (M.Sc. Thesis), Universidad de Chile, Departamento de Geología, Santiago.
- Natland, M., González, E., Canon, A., Ernst, M., 1974. A system of stages for correlation of Magallanes Basin sediments. *Geol. Soc. Am. Mem.* 39 (126 pp.).
- O'Gorman, J.P., Gasparini, Z., Reguero, M., 2010. *Aristonectes parvidens* Cabrera (Sauropterygia, Plesiosauria) from Cape Lamb, Vega Island (Upper Cretaceous), Antarctica. Scientific Committee on Antarctic Research (SCAR), Open Science Conference, No. 31, Abstract 557, Buenos Aires (1 pp.).
- Otero, R., Oyarzún, J.-L., Soto-Acuña, S., Yury-Yáñez, R.E., Gutiérrez, N.M., Le Roux, J.P., Torres, T., Hervé, F., 2013. Neoselachians and Chimaeriformes (Chondrichthyes) from the latest Cretaceous–Paleogene of Sierra Baguales, southernmost Chile. Chronostratigraphic, paleobiogeographic and paleoenvironmental implications. *J. S. Am. Earth Sci.* 48, 13–30.
- Otero, R.A., Soto-Acuña, S., Salazar, C., Oyarzún, J.-L., 2015. New elasmosaurids (Sauropterygia, Plesiosauria) from the Late Cretaceous of the Magallanes Basin, Chilean Patagonia: evidence of a faunal turnover during the Maastrichtian along the Weddellian Biogeographic Province. *Andean Geol.* 42, 237–267.
- Otero, R.A., Soto-Acuña, S., Vargas, A.O., Rubilar-Rogers, D., Yury-Yáñez, R., Gutstein, C.S., 2014. Additions to the diversity of elasmosaurid plesiosaurs from the Upper Cretaceous of Antarctica. *Gondwana Res.* 26, 772–784.
- Otero, R.A., Suárez, M.E., Le Roux, J.P., 2009. First record of elasmosaurid plesiosaurs (Sauropterygia: Plesiosauria) in upper levels of the Dorothea Formation, Late Cretaceous (Maastrichtian), Puerto Natales, Chilean Patagonia. *Andean Geol.* 36, 342–350.
- Pankhurst, R.J., 1990. The Paleozoic and Andean magmatic arcs of West Antarctica and southern South America. *Geol. Soc. Am. Spec. Pap.* 241, 1–7.
- Pankhurst, R.J., Rapela, C.W., 1995. Production of Jurassic rhyolite by anatexis of the lower crust of Patagonia. *Earth Planet. Sci. Lett.* 134, 23–36.
- Pankhurst, R.J., Leat, P.T., Sruoga, P., Rapela, C.W., Marquez, M., Storey, B.C., Riley, T.R., 1998. The Chon Aike province of Patagonia and related rocks in West Antarctica: a silicic large igneous province. *J. Volcanol. Geotherm. Res.* 81, 113–136.
- Pankhurst, R.J., Riley, T.R., Fanning, C.M., Kelley, S.P., 2000. Episodic silicic volcanism in Patagonia and Antarctic Peninsula: chronology of magmatism associated with the breakup of Gondwana. *J. Petrol.* 41, 605–625.
- Parras, A., Dix, G.R., Griffin, M., 2012. Sr-isotope chondrostratigraphy of Paleogene–Neogene marine deposits: Austral Basin, southern Patagonia (Argentina). *J. S. Am. Earth Sci.* 37, 122–135.
- Paulcke, W., 1907. Die Cephalopoden de oberen Kreide Südpatagoniens. *Berichte der Naturforschenden Gesellschaft zu Freiburg* 15, pp. 1–82.
- Pelayo, A.M., Wiens, D.A., 1989. Seismotectonics and relative plate motion in the Scotia sea region. *J. Geophys. Res.* 94, 7293–7320.
- Peppe, D.J., Royer, D.L., Cariglino, B., Oliver, S.Y., Newman, S., Leight, E., Enikolopov, G., Fernandez-Burgos, M., Herrera, F., Adams, J.M., Correa, E., Currano, E.D., Erickson, J.M., Hinojosa, L.F., Hoganson, J.W., Iglesias, A., Jaramillo, C.A., Johnson, K.R., Jordan, G.J., Kraft, N.J.B.V., Lovelock, E.C., Lusk, C.H., Niinemets, Ü., Peñuelas, J., Rapson, J., Wing, S.L., Wright, I.J., 2011. Sensitivity of leaf size and shape to climate: global patterns and palaeoclimatic applications. *New Phytol.* 190, 724–739.
- Permyu Vidal, C., Moreira, P., Guido, D.M., Fanning, C.M., 2014. Linkages between the southern Patagonia Pre-Permian basements: new insights from detrital zircons U-Pb SHRIMP ages from the Cerro Negro District. *Geol. Acta* 12, 137–150.
- Piatnitzky, A., 1938. Observaciones geológicas en el oeste de Santa Cruz (Patagonia). *Boletín de Informaciones Petroleras* 165, pp. 45–85.
- Poblete, F., Arriagada, C., Roperch, C., Astudillo, N., Hervé, F., Kraus, S., Le Roux, J.P., 2011. Paleomagnetism and tectonics of the South Shetland Islands and the northern Antarctic Peninsula. *Earth Planet. Sci. Lett.* 302, 299–313.
- Quattrocchio, M., Martínez, M., Hinojosa, L.F., Jaramillo, C., 2013. Quantitative analysis of Cenozoic palynofloras from Patagonia (southern South America). *Palynology* 37, 246–258.
- Ramos, V.A., 2005. Seismic ridge subduction and topography. Foreland deformation in the Patagonian Andes. *Tectonophysics* 399, 73–86.
- Ramos, V.A., 2008. Patagonia: a Paleozoic continent adrift? *J. S. Am. Earth Sci.* 26, 235–251.
- Ramos, V.M., Kay, S.M., 1992. Southern Patagonian plateau basalts and deformation: back-arc testimony of ridge collisions. *Tectonophysics* 205, 261–282.
- Ramos, V.A., Chemale, F., Naipauer, M., Pazos, P.J., 2014a. A provenance study of the Paleozoic Ventania System (Argentina): transient complex sources from Western and Eastern Gondwana. *Gondwana Res.* 26, 719–740.
- Ramos, V.A., Litvak, V.D., Folguera, A., Spagnuolo, M., 2014b. An Andean tectonic cycle: from crustal thickening to extension in a thin crust (34°–37°S). *Geosci. Front.* 5, 351–367.
- Reguero, M., Goin, F.J., Acosta Hospitaleche, C., Dutra, T., Marensi, S., 2013. West Antarctica: TECTONICS and paleogeography. Late Cretaceous/Paleogene West Antarctica Terrestrial Biota and Its Intercontinental Affinities. *Springer Briefs in Earth System Sciences*, pp. 10–17.
- Riccardi, A.C., Rolleri, E.O., 1980. Cordillera Patagonia Austral. Segundo Simposio Geológico Regional Argentino, Córdoba, pp. 1163–1306.

- Romans, B., Fildani, A., Graham, S., Hubbard, S., 2010. Importance of predecessor basin history on the sedimentary fill of a retroarc foreland basin: provenance analysis of the Cretaceous Magallanes Basin, Chile (50–52°S). *Basin Res.* 22, 640–658.
- Ruddiman, W.F., Raymo, M.E., Prell, W.L., Kutzbach, J.E., 1997. The uplift-climate connection: a synthesis. In: Ruddiman, W.F. (Ed.), *Tectonic Uplift and Climate Change*. Plenum Press, New York, pp. 383–397.
- Sánchez, A., Pavlishina, P., Godoy, E., Hervé, F., Fanning, C.M., 2010. On the presence of Upper Paleocene rocks in the foreland succession at Cabo Nariz, Tierra del Fuego, Chile: geology and new palynological and U-Pb data. *Andean Geol.* 37, 413–432.
- Santos, J.O., Hartmann, L.A., Bossi, J., Campal, N., Schipilov, A., Pifieiro, McNaughton, N.J., 2003. Duration of the TransAmazonian Cycle and its correlation within South America based on U-Pb SHRIMP geochronology of the La Plata craton, Uruguay. *Int. Geol. Rev.* 45, 27–48.
- Scher, H.D., Martin, E.E., 2006. Timing and climatic consequences of the opening of the Drake Passage. *Science* 312, 428–430.
- Schwartz, T.M., Graham, S.A., 2015. Stratigraphic architecture of a tide-influenced shelf-edge delta, Upper Cretaceous Dorotea Formation, Magallanes-Austral Basin, Patagonia. *Sedimentology* 62, 1039–1077.
- Schwartz, T.M., Fosdick, J.C., Graham, S.A., 2016. Using detrital zircon U-Pb ages to calculate Late Cretaceous sedimentation rates in the Magallanes-Austral Basin, Patagonia. *Basin Res.* <http://dx.doi.org/10.1111/bre.12198>, 1–22.
- Scott, K.M., 1966. Sedimentology and dispersal pattern of a Cretaceous flysch sequence, Patagonian Andes, southern Chile. *AAPG Bull.* 50, 72–107.
- Seton, M., Müller, R.D., Zahirovic, S., Gaiña, C., Torsvik, T., Shephard, G., Talsma, A., Gurnis, M., Turner, M., Maus, S., Chandler, M., 2012. Global continental and ocean basin reconstructions since 200 Ma. *Earth Sci. Rev.* 113, 212–270.
- Spicer, R.A., 2000. Leaf physiognomy and climate change. In: Culver, S.J., Rawson, P. (Eds.), *Biotic Response to Global Change: The Last 145 million Years*. Cambridge University Press, Cambridge, pp. 244–264.
- Spicer, R.A., Herman, A.B., Kennedy, E.M., 2004. Foliar physiognomic record of climatic conditions during dormancy: Climate Leaf Analysis Multivariate Program (CLAMP) and the cold month mean temperature. *J. Geol.* 112, 685–702.
- Storey, B.C., Nell, P.A.R., 1988. Role of strike-slip faulting in the tectonic evolution of the Antarctic Peninsula. *J. Geol. Soc. Lond.* 145, 333–337.
- Thomas, C., Livermore, R., Pollitz, F., 2003. Motion of the Scotia Sea plates. *Geophys. J. Int.* 155, 789–804.
- Torres, T., Cisterna, M., Llanos, A., Galleguillos, H., Le Roux, J.P., 2009. Nuevos registros de *Nothofagus* Bl. en Sierra Baguales, Última Esperanza, Patagonia, Chile. Extended Abstracts, XII Congreso Geológico Chileno, Santiago, Chile, pp. S12–S19.
- Ugalde, R.A., 2014. Contribución al conocimiento de la estratigrafía cenozoica de la Sierra Baguales: la formación Man Aike (“Las Flores”). Provincia de Última Esperanza, Magallanes. Memoria de Título. Universidad de Chile (82 pp.).
- Uhl, D., Klotz, S., Traiser, C., Thiel, C., Utescher, T., Kowalski, E., Dilcher, D.L., 2007. Cenozoic paleotemperatures and leaf physiognomy – a European perspective. *Palaeogeogr. Palaeoclimatol. Palaeoecol.* 248, 24–31.
- Veevers, J.J., Powell, C.M.A., Collinson, J.W., López-Gamundí, O.R., 1984. Synthesis. In: Veevers, J.J., Powell, C.M.A. (Eds.), *Permian-Triassic Pangean Basins and Foldbelts along the Pantalassian Margin of Gondwanaland*. Geological Society, America, Memoir Vol. 184, pp. 331–352.
- Wilf, P., 1997. When are leaves good thermometers? A new case for leaf margin analysis. *Paleobiology* 23, 373–390.
- Wilf, P., Johnson, K.R., Cúneo, N.R., Smith, M.E., Singer, B.S., Gandolfo, M.A., 2005. Eocene plant diversity at Laguna del Hunco and Río Pichileufú, Patagonia, Argentina. *Am. Nat.* 165, 634–650.
- Wolfe, J.A., 1993. A method of obtaining climatic parameters from leaf assemblages. *U.S. Geol. Surv. Bull.* 2040, 1–71.
- Wolfe, J.A., 1995. Paleoclimatic estimates from Tertiary leaf assemblages. *Annu. Rev. Earth Planet. Sci.* 23, 119–142.
- Wolfe, J.A., Spicer, R.A., 1999. Fossil leaf character states: multivariate analysis. In: Jones, T.P., Rowe, N.P. (Eds.), *Fossil Plants and Spores: Modern Techniques*. Geological Society, London, pp. 233–239.
- Zachos, J., Pagani, H., Sloan, L., Thomas, E., Billups, K., 2001. Trends, rhythms, and aberrations in global climate: 65 Ma to present. *Science* 292, 686–693.
- Zachos, J.C., Quinn, T.M., Salamy, S., 1996. High-resolution (104 years) deep-sea foraminiferal stable isotope records of the Eocene-Oligocene climate transition. *Paleoceanography* 11, 251–266.
- Zahid, K., Barbeau Jr., D.L., 2010. Provenance of eastern Magallanes foreland basin sediments: heavy mineral analysis reveals Paleogene tectonic unroofing of the Fuegian Andes hinterland. *Sediment. Geol.* 229, 64–74.